Aus der Anatomischen Anstalt der Ludwig-Maximilians-Universität München
Lehrstuhl I - Vegetative Anatomie
Vorstand: Prof. Dr. med. Jens Waschke

The localization and complete extent of the newly defined preganglionic Edinger-Westphal nucleus (EWpg) in human

Dissertation
zum Erwerb des Doktorgrades der Medizin
an der Medizinischen Fakultät der
Ludwig-Maximilians-Universität zu München

vorgelegt von
Laura Ioana Valeanu
aus
Sibiu, Rumänien
Jahr
2020

Mit Genehmigung der Medizinischen Fakultät

der Universität München

Berichterstatter:	Prof. Dr. med. Jens Waschke
Mitberichterstatter:	Prof. Dr. Stefan Glasauer PD Dr. Christoph Trumm
Mitbetreuung durch die promovierte Mitarbeiterin:	Prof. Dr. rer. nat. Anja Horn-Bochtler
Dekan:	Prof. Dr. med. dent. Reinhard Hickel
Tag der mündlichen Prüfung:	19.05.2020

Table of contents

Table of figures

Abbreviations

AM:	anteromedian nucleus
BSA:	bovine serum albumin
CCN:	central caudal nucleus
CG:	ciliary ganglion
ChAT:	choline acetyltransferase
cMRF:	central mesencephalic reticular formation
EW:	Edinger-Westphal nucleus
EWcp:	central projecting part of EW
EWpg:	preganglionic neurons of EW
INC:	interstitial nucleus of Cajal
IO:	inferior oblique muscle
IR:	inferior rectus muscle
LR:	lateral rectus muscle
MIF:	multiply-innervated muscle fibre
MR:	medial rectus muscle
NII:	optic nerve
NIII:	oculomotor nerve
nIII:	oculomotor nucleus
nIV:	trochlear nucleus
nVI:	abducens nucleus
NP-NF:	non-phosphorylated neurofilaments
PBS:	phosphate buffer solution
RN:	red nucleus
RT:	room temperature
SIF:	singly-innervated muscle fibre
SO:	superior oblique muscle
SR:	superior rectus muscle
TBS:	tris buffered saline
UCN:	urocortin

ABSTRACT

Traditionally the Edinger-Westphal nucleus (EW) was considered as the location of preganglionic neurons of the ciliary ganglion (CG) to mediate pupillary constriction and lens accommodation, but was recently shown to refer to two different functional cell groups. Accordingly, a new nomenclature was introduced: In human the cytoarchitecturally defined EW consists of centrally projecting urocortin-positive neurons, which are involved in stress related function, regulation of alcohol and food consumption, is now termed EWcp. In contrast, the preganglionic neurons of the CG are found as an inconspicuous group of cholinergic neurons dorsally, which is now termed EWpg (Kozicz et al. 2011).

In this study the complete population and distribution of cholinergic preganglionic neurons was investigated by immunolabelling for choline acetyltransferase and delineated from urocortin-positive neurons.

Brainstem tissue from five human cases was immersion-fixed in 4% paraform aldehyde and blocks of the midbrain were embedded in paraffin.

Series of adjacent transverse midbrain sections through the whole extent of the oculomotor nucleus complex were immunostained for either choline acetyltransferase (ChAT), urocortin (UCN) or non-phosphorylated neurofilament (NP-NF). The distribution of ChAT-positive preganglionic neurons and UCN-positive central projecting neurons was plotted. Preganglionic neurons were delineated from motoneurons of multiply-innervated muscle fibers of extraocular muscles by their additional expression of NP-NF-immunoreactivity.

In accordance to previous studies preganglionic neurons were found dorsally to EWcp as an inconspicuous group throughout the length of the rostral half of the oculomotor nucleus. In addition another small group of putative preganglionic neurons was found ventral to the oculomotor nucleus not previously described. At rostral planes, UCN-positive and preganglionic neurons are found intermingled within the anteromedian nucleus.

The findings of this study may serve as basis for pathological post-mortem studies of neurodegenerative diseases affecting the pupillary system as suspected for Alzheimer's disease.

ZUSAMMENFASSUNG

Traditionell wird der Edinger-Westphal-Kern (EW) als Sitz der parasympathischen präganglionären Neurone des Ciliarganglions zur Vermittlung der Pupillenkonstriktion und Akkommodation der Linse angesehen. Kürzlich wurde jedoch gezeigt, dass dieser Kern sich auf zwei verschiedene funktionelle Zellgruppen bezieht. Dementsprechend wurde eine neue Nomenklatur eingeführt: Im Menschen besteht der zytoarchitektonisch definierte EW aus zentral projizierenden Urocortin-positiven Neuronen, die an der Stressfunktion und der Anpassung an Alkoholkonsum sowie dem Essverhalten beteiligt sind, somit wurde dieser EWcp genannt. Im Gegensatz dazu finden sich die präganglionären Neurone des Ciliarganglions als eine unauffällige Gruppe von cholinergen Neuronen dorsal davon, die nun EWpg genannt wird (Kozicz et al. 2011).

In dieser Studie wurde mittels immunhistochemischer Färbung für Cholinacetyltransferase die vollständige Population und Verteilung von cholinergen präganglionären Neuronen untersucht und von Urocortin-positiven Neuronen abgegrenzt.

Menschliches Hirnstammgewebe von fünf Fällen wurde in 4% Paraformaldehyd fixiert und Blöcke des Mittelhirns wurden in Paraffin eingebettet.

Serien benachbarter transversaler Mittelhirnschnitte durch den gesamten Bereich des Okulomotoriuskern-Komplexes wurden entweder für Cholinacetyltransferase (ChAT), Urocortin (UCN) oder nicht-phosphoryliertes Neurofilament (NP-NF) immungefärbt. Die Verteilung von ChAT-positiven präganglionären Neuronen und UCN-positiven zentral projizierenden Neuronen wurde geplottet. Anhand ihrer zusätzlichen Expression von NP-NF-Immunreaktivität, konnten die präganglionären Neuronen von Motoneuronen der multipel-innervierten Muskelfasern der äußeren Augenmuskeln abgegrenzt werden.

In Übereinstimmung mit früheren Studien wurden präganglionäre Neurone als unauffällige Gruppe dorsal zu Ewcp, über die gesamte Länge der rostralen Hälfte des Okulomotoriuskerns gefunden. Daneben wurde eine weitere kleine Gruppe von mutmaßlichen präganglionären Neuronen ventral des Okulomotoriuskernes lokalisiert, die zuvor nicht beschrieben wurde. In rostralen Ebenen fanden sich UCN-positive und präganglionäre Neuronen im Anteromedianen Kern miteinander gemischt.

Die Ergebnisse dieser Studie können als Grundlage für pathologische postmortem Studien im Zusammenhang mit neurodegenerativen Erkrankungen die das Pupillensystem beeinflussen, wie im Fall von der Alzheimer-Krankheit vermutet, dienen.

I. INTRODUCTION

I.1. Anatomy and function of the inner eye muscles

Two important functions are subserved by the inner eye muscles: the pupillary light reflex and the lens accommodation. These are controlled by the autonomic nervous system (McDougal and Gamlin, 2015). In this study the focus is pointed on the parasympathetic function of the intrinsic muscles of the eye: the iris sphincter and the ciliary muscle (accommodative apparatus), and their control by the Edinger-Westphal nucleus in the mesencephalon (Kardon, 2005).

I.1.1. The iris sphincter muscle

The iris sphincter muscle is part of the iris and is responsible for pupillary constriction (myosis), thus contributing to the pupillary light reflex with its major function: to maximize visual perception while optimizing retinal illumination (Wilhelm, 2011).

The iris consists of a peripheral ciliary portion and a central pupillary zone, with a collarette between those two zones. The sphincter muscle is located at the pupillary end of the iris and it is concentrically arranged, which means the muscle cells are orientated parallel to the pupillary margin. Farther to the cilliary zone it is bound to a connective tissue that continues to the iris dilator muscle. The dilator muscle is embedded in the anterior epithelium, which is composed of unique myoepithelial cells. The muscle cells are orientated radially from the iris root to the pupillary border and their contraction causes pupil dilation (mydriasis) (Kardon, 2005; see Figures 1 and 2).

I.1.2. The ciliary muscle

When visual fixation is shifted from a far object to a near one, the ciliary muscle modulates the shape of the lens to obtain a clear image of the near object. This reaction is termed accommodation and is part of the near response together with the pupillary constriction and the convergence of the eyes (McDougal and Gamlin, 2015).

This muscle is located in the ciliary body which encircles the anterior inner surface of the eye as a belt and is continuous with the iris anteriorly, while posteriorly it continues with the choroid and with the overlying peripheral retina at the ora serrata (Figure 1).

The ciliary muscle is subdivided in pars plana and pars plicata, both containing three layers: unpigmented ciliary epithelium, pigmented ciliary epithelium and the stroma with the ciliary muscle, which consists of circular, radial, and longitudinal muscle fiber orientations (Figure 2).

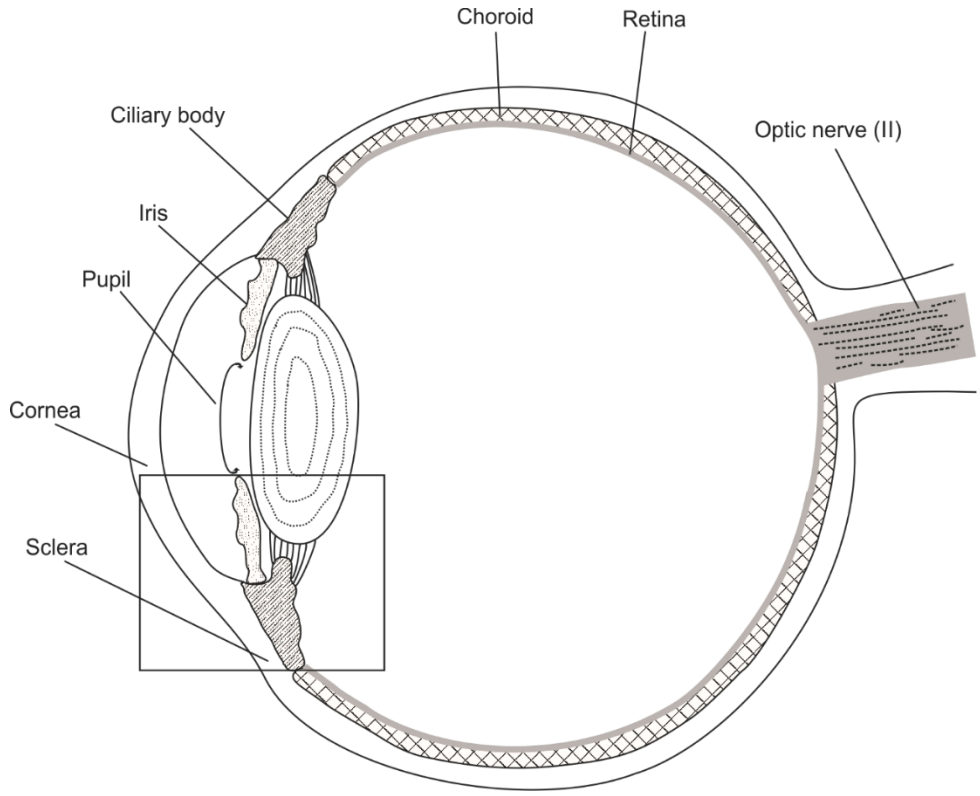

Figure 1. Schematic drawing of a sagittal section through the eyeball showing the anatomical structures relevant for this study.

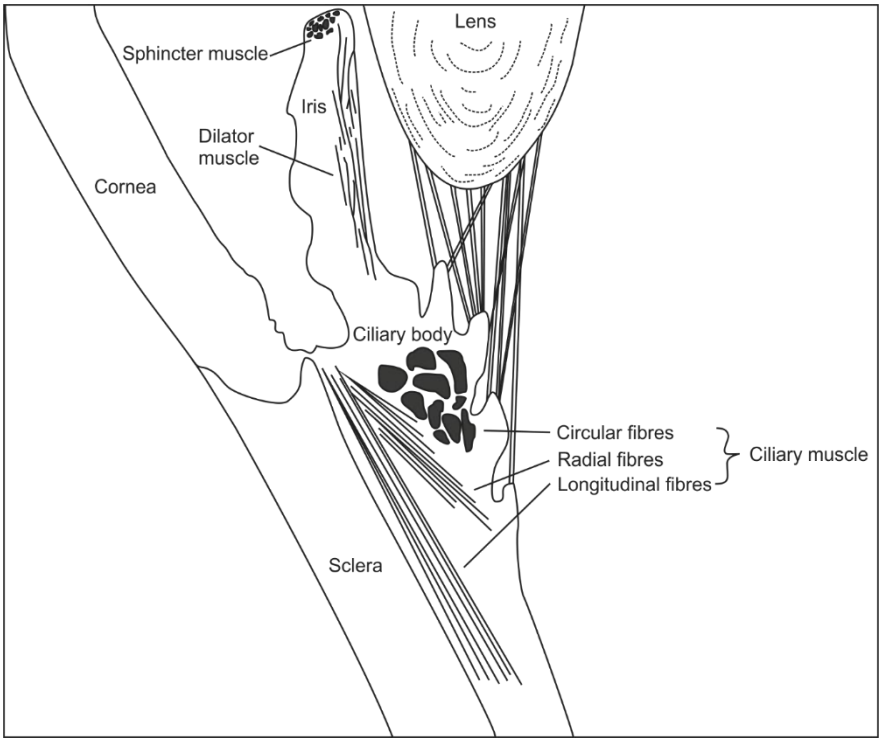

Figure 2. Anatomical scheme of a detailed view of Figure 1 (rectangle).

I.2. Innervation of the inner eye muscles

The smooth muscle cells of the inner eye muscles are innervated by nerve fibres of the autonomic nervous system, which consists of two components: the sympathetic and the parasympathetic system (for review see Gibbins, 2012). Unlike the somatoefferent motoaxons that directly innervate skeletal muscle fibres, the autonomic efferents consist of a two neuron chain:

- preganglionic neurons with origin in the CNS, in the visceral efferent nuclei of cranial nerves (i.e., parasympathetic) or in the lateral horn of the thoracal spinal cord (i.e., sympathetic).
- postganglionic neurons with origin in one of the ganglia outside of the CNS.

Preganglionic neurons, both parasympathetic and sympathetic use acetylcholine as a neurotransmitter. This substance is also expressed by the postganglionic parasympathetic neurons, while, with some exceptions, the sympathetic postganglionic neurons mainly contain the catecholamine norepinephrine (Nieuwenhuys, 1985).

The iris sphincter muscle has at least 20 segments, each innervated in series by separate branches of parasympathetic postganglionic nerves from the ciliary ganglion, whereas the iris dilator muscle is innervated by sympathetic nerve fibres. The ciliary muscle is activated primarily by the mesencephalic, parasympathetic outflow but is also influenced by cervical sympathetic outflow (Kardon, 2005).

Since the present study addresses the organization of the preganglionic neurons in the Edinger-Westphal nucleus, only the parasympathetic innervation of the inner muscles is described in the following sections, referring to the EWpg (preganglionic neurons) and the CG (postganglionic neurons).

Parasympathetic pathways related to EW nucleus control pupillary constriction and lens accommodation (Gibbins, 2012). Two ocular reflexes are related to pupillary constriction: the pupillary light reflex and the pupillary near response reflex, the last one being additionaly related to accommodation and convergence (McDougal and Gamlin, 2015).

The postganglionic neurons of these pathways are located in the CG. Their preganglionic impulses are carried from the EWpg in the midbrain and synapse within the CG via the oculomotor nerve (NIII) (Wilhelm, 2011). The CG is an irregular structure, which is located in the orbital fat behind the ophthalmic globe (Gibbins,

2012). The axons of the postganglionic neurons exit the CG and travel via the short ciliary nerves towards the ocular globe to innervate the iris sphincter and the ciliary muscle (see Figures 3 and 4). This is the common efferent pathway for both reflexes mentioned above.

The afferent pathway of the pupillary light reflex carries impulses from the retinal cells to the pretectal area in the dorsal midbrain via the optic nerve (NII). From the pretectum the signal reach the EWpg (Wilhelm, 2011). The afferent inputs of the pupillary near response are more complex and involve the visual pathway in the interplay with accommodation (for review see McDougal and Gamlin, 2015). However, these two reflexes intersect at the EWpg and it is generally accepted that the neurons within EWpg drive the pupillary light reflex and the pupillary near reflex, including the lens accommodation (McDougal and Gamlin, 2015).

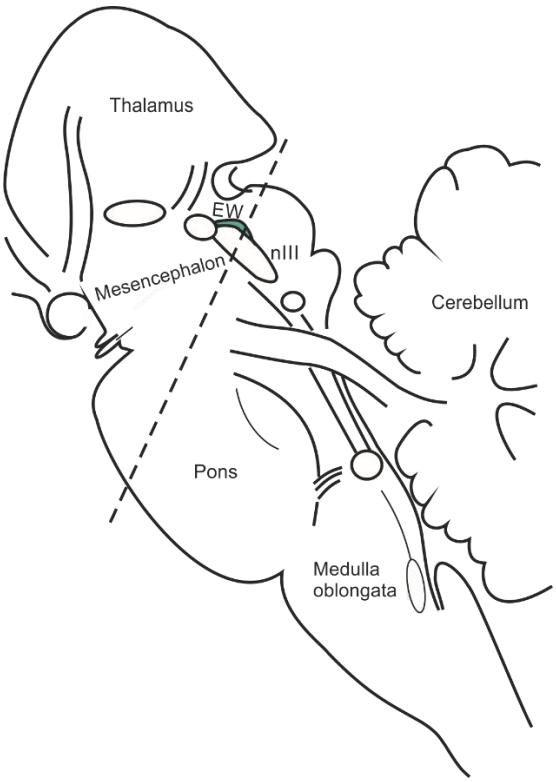

Figure 3. Schematic drawing of a sagittal view of the human brainstem showing the cutting plane for Figure 4.

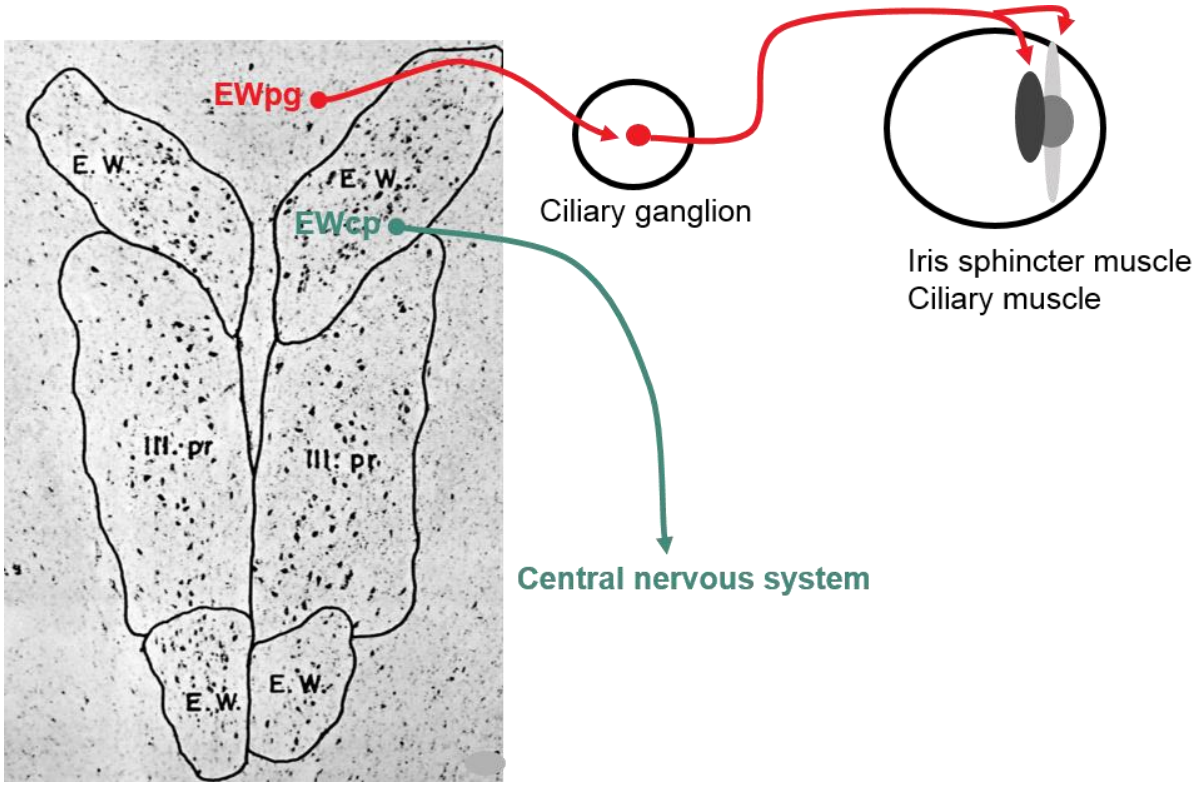

Figure 4. Transverse Nissl-stained section of the oculomotor nucleus complex to demonstrate the cytoarchitecture of functional cell groups of the Edinger-Westphal nucleus (EW) with preganglionic neurons (EWpg) and central projecting neurons (EWcp). With permission from Karger. Adopted from Olszewski, J. (Montreal, QC) and Baxter, D. (Montreal, QC), Cytoarchitecture of the Human Brain Stem, 2nd unchanged edition 1982. Copyright S. Karger AG, Basel (page 97, modified Figure 4).

I.3. Motoneurons of extraocular muscles

The motor innervation of the extraocular muscles is controlled by three nuclei areas in the brainstem. The motoneurons of the lateral rectus muscle (LR) are located in the abducens nucleus (nVI), those of the superior oblique muscle (SO) in the trochlear nucleus (nIV) and those of all the other extraocular muscles lie in the oculomotor nucleus (nIII) (Sharpe and Wong, 2005).

Extraocular muscles present an abundance of different muscle fibre types, which can be divided in two main groups by their innervation pattern (Spencer and Porter, 2006): twitch muscle fibers innervated by a single en-plaque nerve ending (SIF) and non-twitch muscle fibers targeted by multiple small en-grappe endings along the whole muscle fiber extent (MIF). In accordance with that, two types of motoneurons can be distinguished. These motoneurons differ in their location (Büttner-Ennever et al.,

2001), their afferent input (Wasicky et al., 2004) and their histochemical properties (Eberhorn et al., 2005). Whereas SIF-motoneurons are located within the boundaries of the oculomotor (nIII), trochlear (nIV) and abducens (nVI) nuclei and express non-phosphorylated neurofilaments (NP-NF), MIF-motoneurons lie in the periphery of the motonuclei and lack NP-NF (Eberhorn et al., 2005).

The SIF motoneurons may generate the eye movement, while the MIF motoneurons are thought to play a role in controlling the tension in the extraocular muscle during vergence and eye alignment during fixation (Büttner-Ennever, 2006; Büttner-Ennever and Horn, 2014).

I.4. Oculomotor nucleus complex

The oculomotor nucleus complex with its perioculomotor region is composed of cytoarchitecturally and functionally different cell groups containing somatic and visceral nuclei (Parent, 1996). The nuclei nIII, CCN, NP, EWpg and part of AM consist of cholinergic motoneurons, innervating extraocular and inner eye muscles and also the levator palpebrae, being related to external stimuli. Whereas the nuclei EWcp and part of AM contain peptidergic non-motor neurons projecting centrally and being linked to internal stimuli (e.g. stress) (Kozicz et al., 2011).

The **oculomotor nucleus (nIII)** constitutes the major component of the oculomotor nucleus complex. It contains subgroups of motoneurons supplying 4 extraocular eye muscles: the contralateral superior rectus (SR), the ipsilateral medial rectus (MR), inferior rectus (IR) and inferior oblique (IO). Their axons travel to the orbit in the oculomotor nerve (NIII) (Che Ngwa et al., 2014).

At caudal level of nIII the **caudal central nucleus (CCN)** is located between the two parts of this nucleus at the midline. It supplies the two levator palpebrae superioris muscles which raise both eye lids via the oculomotor nerve (Büttner-Ennever and Horn, 2004).

Also between the two parts of nIII, but farther rostrally the **nucleus of Perlia (NP)** can be found. This nucleus is present in 80% of humans and its degree of development varies from individual to individual (Tsuchida, 1906). The function of NP is not known yet, but based on histochemical and morphological properties, its neurons are presumed twitch-motoneurons that supply SIFs within extraocular muscles (Horn et al., 2008; Che Ngwa et al., 2014). Che Ngwa et al., 2014 brings a new point in, suggesting a Calretinin (CR) input to this subgroup and presuming the NP may

represent superior rectus muscle SIF motoneurons that were separated from the adjacent main nIII by dorsoventrally travelling axons, being involved in upgaze.

Also part of the perioculomotor region are the cholinergic **MIF motoneurons**, which lack NP-NF and were described around the dorsomedial and ventral border of the nIII in human (Horn et al., 2008), but a precise localization and extension is yet unknown.

Dorsally, dorsomedially and ventrally the nIII is embraced by **the traditional Edinger-Westphal nucleus**, which forms a cytoarchitectural entity (Olszewski and Baxter's, 1982). This cell group of small densely packed neurons has been considered as the preganglionic neurons of the ciliary ganglion for more than 100 years. After the discovery of the neuropeptide urocortin and the description of its localization in the EW (Vaughan et al., 1995), systematic investigations in different species did reveal the dilemma that the cytoarchitecturally defined EW refers to two functionally distinct cell groups across species: cholinergic preganglionic neurons that project into the periphery via the ciliary ganglion and mediate pupillary constriction and accommodation of the lens, and peptidergic neurons that project to other centers within the brain and play a role in adaptation to stress, eating habits and alcohol consumption (Kozicz et al., 2011). It was also found that the EW in human express immunoreactivity for urocortin and not for the expected transmitter acetylcholine (Ryabinin et al., 2005; Horn et al., 2008).

Considering the cytoarchitecture, histochemistry and function of different cell groups within the perioculomotor area, a new more specific nomenclature for functional cell groups was introduced. This includes the parasympathetic preganglionic neurons, now termed EWpg and the UCN-positive centrally projecting neurons, newly termed EWcp (Kozicz et al., 2011).

In order to perform correlated clinico-anatomical post mortem studies of clinical cases with neurodegenerative diseases affecting pupillary response, the exact location, extent and delineation from other adjacent cell groups is crucial.

I.5. Aim of the study

Based on the recent discover, that the preganglionic parasympathetic neurons for pupil constriction and lens accommodation are not located in the classical cytoarchitecturally defined EW in human, but are located dorsally as an inconspicuous cell group, which was not systematically investigated, the present thesis addresses the following questions:

1. What is the distribution of the complete population of cholinergic preganglionic parasympathetic neurons in human? Is there a compact portion of putative preganglionic neurons along its caudorostral extension forming the homologue of the EWpg in monkey?

2. What is the spatial relationship between preganglionic neurons of the EWpg and the peptidergic neurons of the EWcp throughout the mesencephalon?

For delineation, series of neighbouring transverse paraffin brainstem sections from human control cases were stained with immunoperoxidase methods for the visualization of either ChAT or UCN. For the discrimination between MIF motoneurons in the periphery of nIII and putative preganglionic neurons, additional neighbouring sections were immunostained for NP-NF, which is expressed in preganglionic neurons (as SIF-motoneurons), but not MIF motoneurons (Horn et al., 2008).

II. MATERIAL AND METHODS

II.1. Cases

To investigate the exact topographical location and the complete extent of the EWpg in human, paraffin-embedded midbrain sections of five post mortem human control cases were used. The cases were obtained 24-72 h after death through the Reference Center for Neurodegenerative Disorders of the Ludwig-Maximilians University with written consent from next of kin, who confirmed the wishes at time of death. The Local Research Ethics Committees approved all procedures. The study is in accordance with the ethical standards laid down in the Declaration of Helsinki, 1964.

The age of the donors ranged from 62-75 years and they had not suffered from any neurological diseases. The stage I pathology for Alzheimer's disease ist still considered as control, since no clinical symptoms are evident in this stage.

Case 1 was a 67-year-old male with rectal cancer, who died of heart failure and, whose neuropathological examination showed old infarcts in the right occipital and frontal lobe.

Case 2 was a 75-year-old male with arteriosclerosis, who died of cardiac infarction.

Case 3 was a 71-year-old male, who died of multiple organ failure due to cardiogenic shock, suffering from congestive heart failure and acute bronchopneumonia. The neuropathological examination demonstrated considerable arteriosclerosis with mild stenosis of brainstem vessels and mild frontal and temporal lobe atrophy.

Case 4 was a 75-year-old female, who died of septic shock due to pneumonia. The neuropathological examination demonstrated subcortical arteriosclerotic encephalopahthy, an old, small infarction in the occipital white matter, considerable arteriosclerosis of the cerebral vessels and stage I Alzheimer.

Case 5 was a 62-year-old male who died of hepatic metastatic pancreatic cancer. There were no brain metastases or an hepatic encephalopathy. The neuropathological examination revealed small old hemorrhages in the adenohypophysis, arteriosclerosis and stage I Alzheimer.

Case	Age,Gender	Cause of death	Post-mortem delay (hours)	Fixation duration (days)
1	67, male	Cardiogenic shock	24	10
2	75, male	Cardiac infarction	72	10
3	71, male	Cardiogenic shock	24	7
4	75, female	Septic shock	24	2
5	62, male	Pacreatic cancer	24	6

Table 1. Human post-mortem paraffin cases used in the study.

II.2. Preparing the sections

The tissue was immersion-fixed in 4% paraform aldehyde for 7-10 days. Blocks of the midbrain were embedded in paraffin and transversal sections (different cutting angles, Case 4 with an almost horizontally cutting plane) of 10 µm thickness from Case 1 and serial sections of 7 µm and 10 µm respectively of 5 µm, 10 µm and 20 µm thickness were cut from Case 2 respectively Case 3, 4 and 5. The sections were then mounted on superfrost and gelatine slides.

II.3. Staining

II.3.1. Nissl-staining

Nissl stains the rRNA in the ribosoms of neurons and in the surrounding glial cells in a purple colour.

Approximately every 20th transverse paraffin section of immersion-fixed (4% paraform aldehyde) human brainstems were Nissl-stained (named after the german neuropathologist Franz Nissl, who worked in the Department of Anatomy of the Ludwig Maximilians University in Munich), using 0.5% cresyl violet to create an overview of the cytoarchitecture.

II.3.2. Immunostaining

Neighbouring sections to the Nissl-stained ones were immmunostained with antibodies against Cholineacetyltransferase (ChAT), urocortin (UCN) and non-phosphorylated neurofilaments (NP-NF). Detection of the primary antibody was revealed by

biotinylated secondary antibody and extravidin-peroxidase with a subsequent reaction of DAB and H_2O_2 (see staining protocols).
Immunolabelling for ChAT and NP-NF was used to outline the EWpg motoneurons and to distinguish them from the MIF motoneurons, as the UCN-immunoreactivity was used to delineate the EWcp.

II.3.2.1. Antibodies

Cholineacetyltransferase (ChAT)

Detection of the cholinergic motoneurons was revealed with a polyclonal ChAT antibody raised in goat (AB144P; Chemicon) against the whole enzyme isolated from human placenta, which is identical to the brain enzyme (Bruce et al.,1985). The antibody was previously used in the paper Horn et al. 2008.

Urocortin (UCN)

Peptidergic, urocortin containing neurons were identified with a polyclonal antibody (U-4757; Sigma, Taufkirchen, Germany), which was raised in rabbit using a synthetic peptide corresponding to the C-terminus of human UCN (amino acids 25–40 with N-terminally added lysine). The pattern of immunostaining is identical to that in other descriptions (Vasconcelos et al., 2003; Horn et al., 2008).

Non-phosphorylated neurofilaments (NP-NF)

For the detection of non-phosphorylated neurofilaments, a mouse monoclonal antibody (IgG1) was used, supplied as a high-titer mouse ascites fluid. The antibody was raised against homogenized hypothalami recovered from Fischer 344 rats (Sternberger et al.,1982). It reacts with a nonphosphorylated epitope of neurofilament H. This antibody was used in previous studies (Sternberger and Sternberger, 1983; Horn et al., 2008).

II.4. Immunoperoxidase procedure

After deparaffinization in Xylene, rehydratation in decreasing concentrations of alcohol (100%, 96%, 90% and 70%) and being shortly rinsed in distilled water, the brainstem sections were boiled in 0.01 M sodium citrate buffer pH 8.5 - 9 in a water bath at 80°C for 15 minutes (Jiao et al., 1999). Then, for another 15 minutes incubated at room temperature, before being washed in 0.1 M Tris-Buffered-Saline (TBS; pH 7.6) and treated with 1% H_2O_2 in 0.1 M TBS for 30 minutes to eliminate endogenous peroxidase activity causing background staining. Next, the sections were washed again with TBS,

before preincubating with 5% normal goat serum (for UCN), normal rabbit serum (for ChAT), or normal horse serum (for NP-NF) in 0.3% Triton in 0.1 M TBS for 1 hour at room temperature. After this, the brainstems were treated either with rabbit anti-UCN (1:6,000), goat anti-ChAT (1:50) or mouse anti-NP-NF (1:5,000) and incubated at 4 °C for 48 hours. After being washed in 0.1 M TBS, the sections were incubated in either biotinylated goat anti-rabbit IgG (1:200), biotinylated rabbit anti-goat (1:200), or biotinylated horse anti-mouse IgG (1:200) at room temperature for 1 hour, followed by three washes in 0.1 M TBS and a 1-hour incubation in extravidin-peroxidase (1:1,000; Sigma) at room temperature. After two washes in 0.1 M TBS pH 7,4 and one wash in 0.05 M TBS pH 7,6 the antigenic sites were visualized by a reaction of 0.025% diaminobenzidine and 0.015% H_2O_2 in 0.05 M TBS pH 7,6 for 10 minutes. After completion of the chromogen reaction, the sections were washed three times in TBS and briefly rinsed in distilled water, air dried, dehydrated in increasing concentrations of alcohol (70%, 90%, 96% and 100%) and in Xylene and coverslipped in Depex (Serva, Heidelberg, Germany).

Sources and Dilutions of the antibodies used in the study

Primary antibody	Manufacturer and Cat. No.	Dilution
Polyclonal goat anti - Choline Acetyltransferase / Gt - ChAT	Chemicon, AB-144P	1:50
Polyclonal rabbit anti - Urocortin / Rb-Urn	Sigma, U-4757	1:6000
Monoclonal mouse anti - Neurofilament H Non-Phosphorylated / Ms-SMI32P	Sternberger, SMI-32P	1:5000

Secondary biotinylated antibody	Manufacturer and Cat. No.	Dilution
Rabbit anti-goat	Vector, BA-5000	1:200
Goat anti-rabbit	Vector, BA-1000	1:200
Horse anti-mouse	Vector, BA-2001	1:200

Table 2 and 3. Overview of the primary and secondary antibodies, sources, and dilutions used for immunoperoxidase labelling.

II.5. Analysis of stained sections

Immuno- and Nissl-stained histological sections were scanned with a slide scanner (Mirax Midi, Zeiss) at 20x magnification. The digitized images were then evaluated and processed on the computer screen with the Panoramic Viewer software (version number 1.15.2). Overview and detailed photographs were taken from the digitized images using this software.

For plotting, low magnification photographs of the sections were taken with a digital camera (MBF Bioscience, Imaging Q38232) mounted on a light microscope (Zeiss, Axioplan). The digitized images were stored on a computer and then analysed using an image editing program (Adobe Photoshop Software 6.0.). The sharpness, the contrast and the brightness were adjusted until the image on the computer screen corresponded exactly to the image seen through the microscope.

In neighbouring sections the ChAT- and UCN-positive neurons in the perioculomotor area and within AM were plotted using a drawing software (CorelDraw version 11.0, Corel Coperation, 2002). The same drawing software was used for the preparation of all schemes as well as for the layout and labelling of the figures.

III. RESULTS

III.1. Cytoarchitecture of the oculomotor nucleus complex in human

The **oculomotor nucleus (nIII)** is located in the tegmentum of the midbrain, ventral to the gray matter and the cerebral aqueduct at the level of the superior colliculus. It extends from the rostral pole of the trochlear nucleus (nIV) to the unpaired portion of the nucleus of Edinger-Westphal, the anteromedian nucleus (AM) (Olszewski and Baxter's, 1982), a average distance of approximately 3 mm (see Table 5).

On cross-sections at caudal levels of the nIII the unpaired **caudal central nucleus (CCN)** overlies the paired nIII at the midline (Figure 5A,B). The motoneurons of CCN are similar, but smaller than those of nIII. Farther rostrally at mid-levels of nIII the unpaired **nucleus of Perlia (NP)** appears at the midline between the two nIII (Figure 5C). The charachteristics of the NP-cells are similar to those in nIII featuring prominent Nissl-bodies, but are smaller and spindle-shaped neurons (Büttner-Ennever and Horn, 2014).

Dorsal, dorsomedial and ventral to nIII the components of the cytoarchitecturally outlined **Edinger-Westphal nucleus (EW)** (Olszewski and Baxter's, 1982), which corresponds to **the central-projecting EW (EWcp)** (Kozicz et al., 2011), can be delineated (Figure 5B,C,D,E). Coming from caudal, at the level of the rostral end of CCN, in close proximity to the dorsal border of both nIII, the EWcp appears (Figure 5B). At mid-levels, the EWcp appears as two separate groups, a lateral (Figure 5B) and a medial part (Figure 5C). Up to the rostral end of the nIII, the main nuclei are comprised by the EWcp, appearing as a conspicuous group dorsally with a small ventral prolongation (Figure 5D).

The two parts of EWcp merge at more rostral levels and extend into the area of the **anteromedian nucleus (AM)** (Figure 5E,F). At levels rostral to nIII only the small cells of the AM are visible (Figure 5F). These neurons have a similar morphology to those of the EWcp as they form a rostral extension of this nucleus.

In Nissl-staining, no compact cell group representing **preganglionic neurons of the EWpg** is visible. At close inspection some larger neurons with a motoneuron-like morphology (Figure 6A) are found scattered dorsal to nIII, which could represent the EWpg.

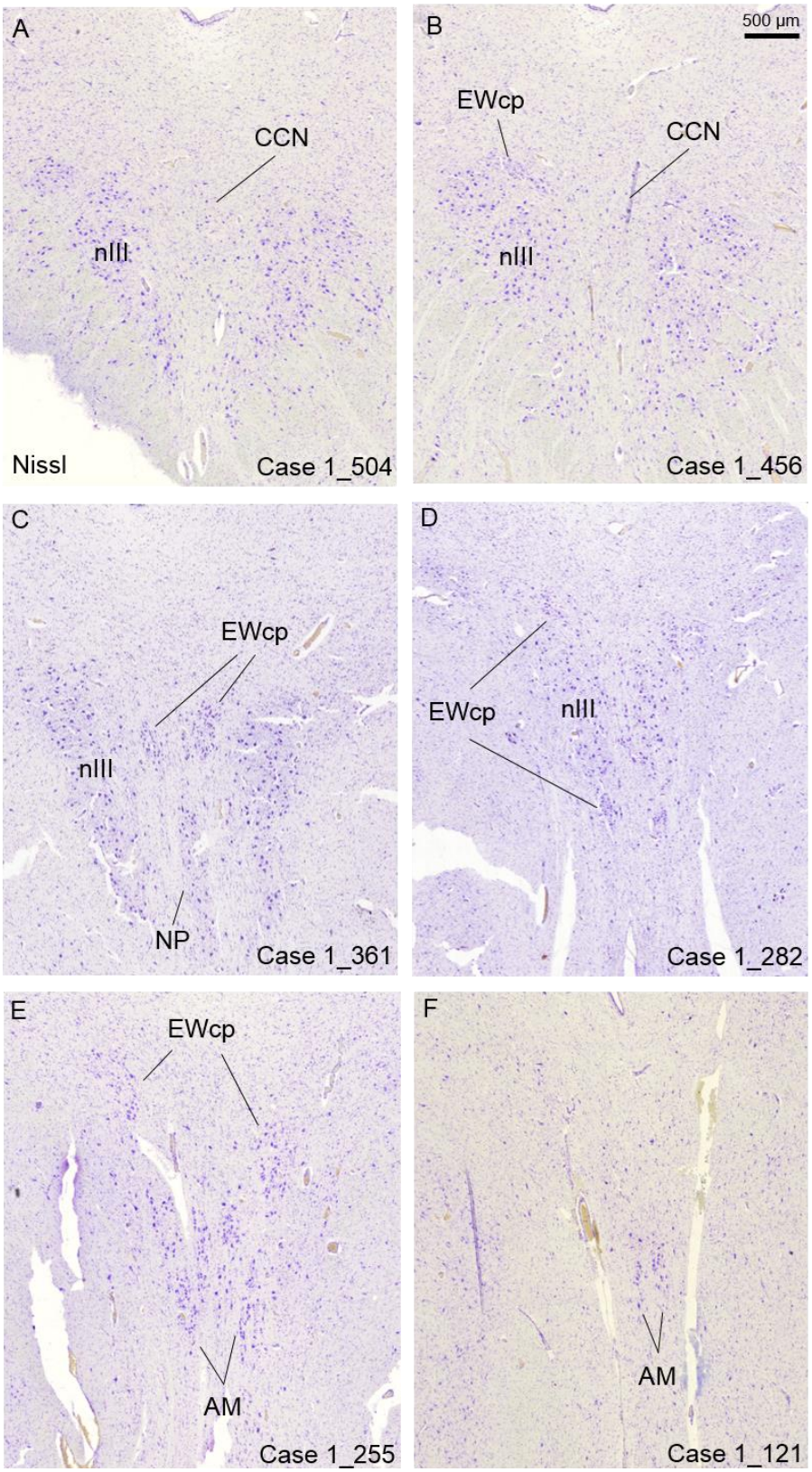

Figure 5. For orientation and demonstration of the cytoarchitecture, this figure shows a series of Nissl-stained transverse sections through the oculomotor nucleus complex from caudal to rostral to create an overview of the perioculomotor cell groups and their topographical relation.

III.2. Delineation of EWpg and EWcp by ChAT- and UCN-immunostaining

Using immunohistochemical markers such as ChAT and UCN, the perioculomotor cell groups of interest could be identified and distinguished from each other and from nIII by differences in their histochemical properties and their morphology (see Figure 6 and Table 4). Parasympathetic preganglionic neurons of the EWpg are ChAT-positive (Figure 6A,B), neurons in the EWcp are UCN-positive and show densly packed UCN-positive granules in their cell bodies (Figure 6C,D). The ChAT-positive motoneurons of extraocular muscles in nIII have a similar morphology to the preganglionic neurons in the EWpg, but the neurons within EWpg are smaller (compare Figures 6A,B with 6E,F). Further more the ChAT-positive, plump neurons within EWpg and nIII are relative isolated (Figure 6A,B,E,F) compared to the UCN-positive neurons within EWcp, which are densly grouped and have a more oval shape (Figure 6C,D).

The UCN-positive neurons, specifically labelled the neurons within the EWcp (Figure 7A,B; 9A,B) and AM (Figure 11A,B) as seen in Nissl-stainings. This includes a large group dorsal to the ChAT-positive neurons of nIII and a small group ventral to nIII (Figure 7B; 9B), as also the peptidergic neurons within AM (Figure 11B).

Neighbouring sections to the UCN-labelled sections, immunostained for ChAT, show some cholinergic neurons scattered within the perioculomotor region (Figure 7C; 9C) and also intermixed with the peptidergic neurons within the AM (Figure 11C).

These ChAT-positive neurons cannot be assigned to a cytoarchitectural entity in Nissl-stained sections and could represent parasympathetic preganglionic motoneurons of the ciliary ganglion (EWpg) or MIF motoneurons.

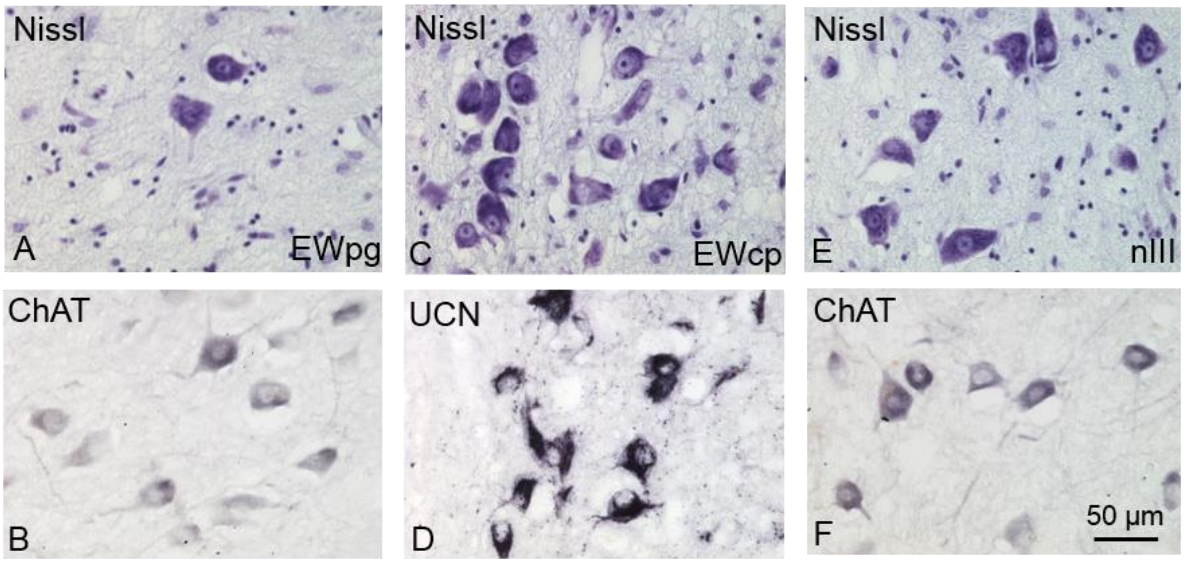

Figure 6. Detailed views of the morphology and immunostaining of the EWpg-, EWcp-group and of the nIII. Both, the motoneurons within nIII (E, F) and the preganglionic neurons in EWpg (A, B) contain prominent, clear Nissl bodies, express ChAT-immunoreactivity and the individual neurons are relative isolated (compare A, B and E, F). In contrast, the densly arranged neurons in the EWcp have a prominent nucleus and the Nissl-substance is packed in clumps near the periphery of the somata (C). The EWcp neurons are not cholinergic, but express UCN (D).

III.3. Delineation of EWpg from MIF motoneurons by NP-NF-immunostaining

As the cholinergic neurons of the EWpg, the MIF motoneurons are also located in the perioculomotor region. These two groups can be distinguished from each other by NP-NF-immunostaining, which is expressed in EWpg neurons, but not in MIF motoneurons (see Table 4) (Horn et al., 2008). Therefore neighbouring sections stained for either ChAT or NP-NF were analysed for colabelling to identify the EWpg neurons.

Besides the classical cholinergic motoneurons of extraocular muscles within nIII, additional cholinergic cell groups were found dorsal to the UCN-positive neurons of the EWcp (Figure 7C; 9C),at the midline between both nIII (Figure 9C) and ventral to the ventral UCN-positive group of EWcp (Figure 7C; 9C). The close inspection of all these peripheral ChAT-positive neurons for the expression of NP-NF in adjacent sections revealed that all ChAT-positive neurons dorsal to the UCN-positive neurons of the EWcp were NP-NF-positive and therefore considered as preganglionic neurons of the EWpg (Figures 7A,C,D; 8A,B; 9A,C,D; 10). In addition, the cholinergic neurons within the cell group ventral to the ventral extension of the UCN-positive EWcp group (Figure 7C,D; 8C,D; 9A,C,D; 10) also express NP-NF-immunoreactivity, and are therefore considered as preganglionic neurons.

The group of smaller ChAT-positive neurons between the nIII and at the dorsomedial border of nIII did not express NP-NF-immunoreactivity (Figure 7C and 9C arrows), and were therefore considered as MIF motoneurons.

At rostral levels ventral to nIII the UCN- and ChAT-immunoreactive neurons appear intermingled within the cytoarchitecturally outlined AM (Figure 11A,B,C). The close analysis of the cholinergic neurons in adjacent sections stained for NP-NF revealed that these represent putative preganglionic neurons as well (Figure 11C,D; 12A,B).

Stain	EWpg	EWcp	nIII	MIF
ChAT	+	-	+	+
UCN	-	+	-	-
NP-NF	+	-	+	-

Table 4. An overview of the markers expressed by the different cell groups within the oculomotor nucleus complex.

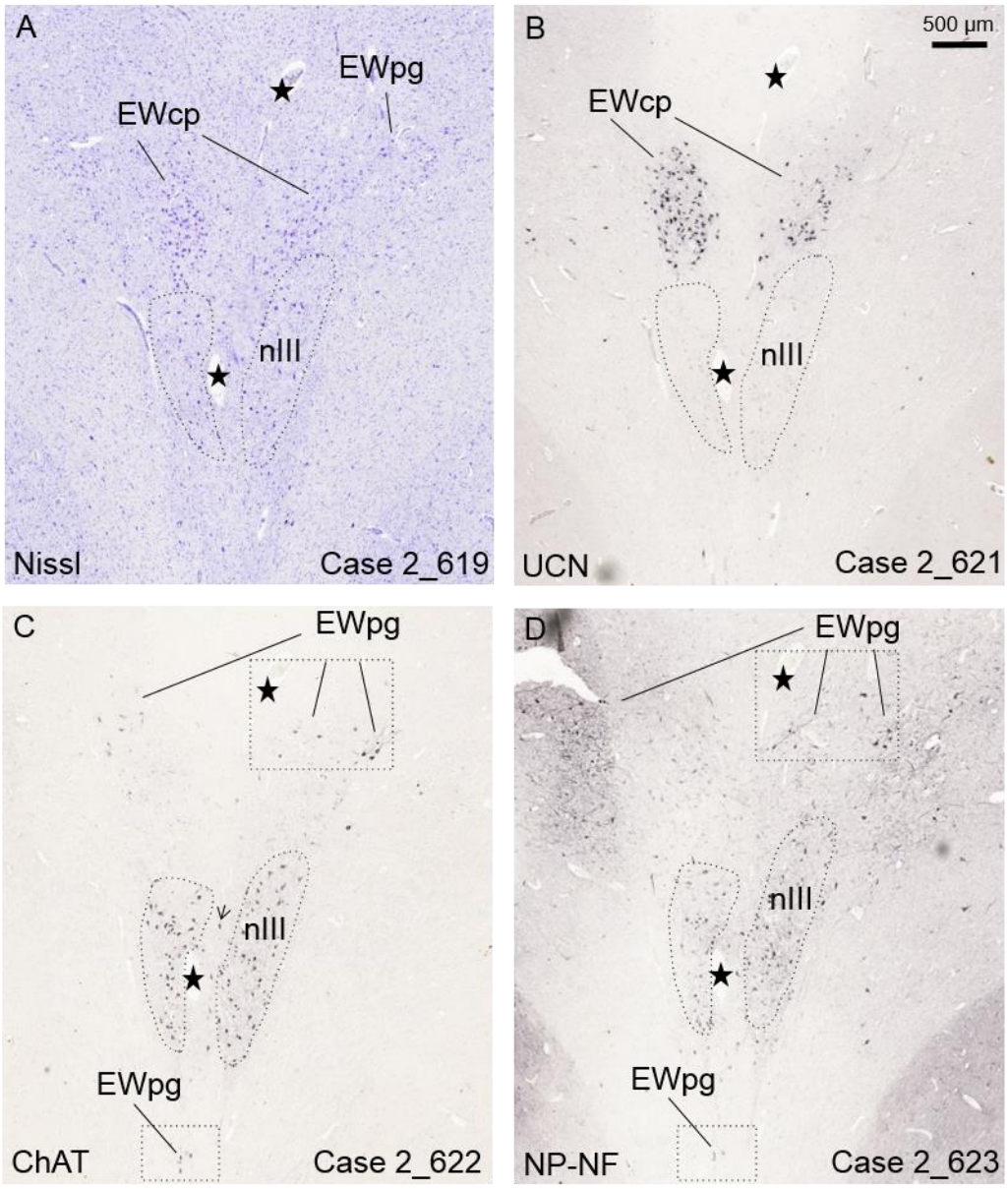

Figure 7. Photographs of neighbouring sections (asterisks in corresponding blood vessels are serving as landmarks) at a rostral level of nIII, corresponding to Figure 14 plane E and stained for Nissl, UCN, ChAT and NP-NF to show the cytoarchitecture (A) and the delineation of EWpg from EWcp (B,C) and MIF neurons (C,D). Extraocular muscle motoneurons within nIII and inner eye muscle preganglionic neurons within EWpg are ChAT- (C) and NP-NF-positive (D), MIF motoneurons are ChAT-positive and lack NP-NF (see arrow in C), neurons of the EWcp are UCN-positve and lack ChAT and NP-NF (B). The squares in C and D mark detailed views of the dorsal and ventral group of EWpg seen in Figure 8.

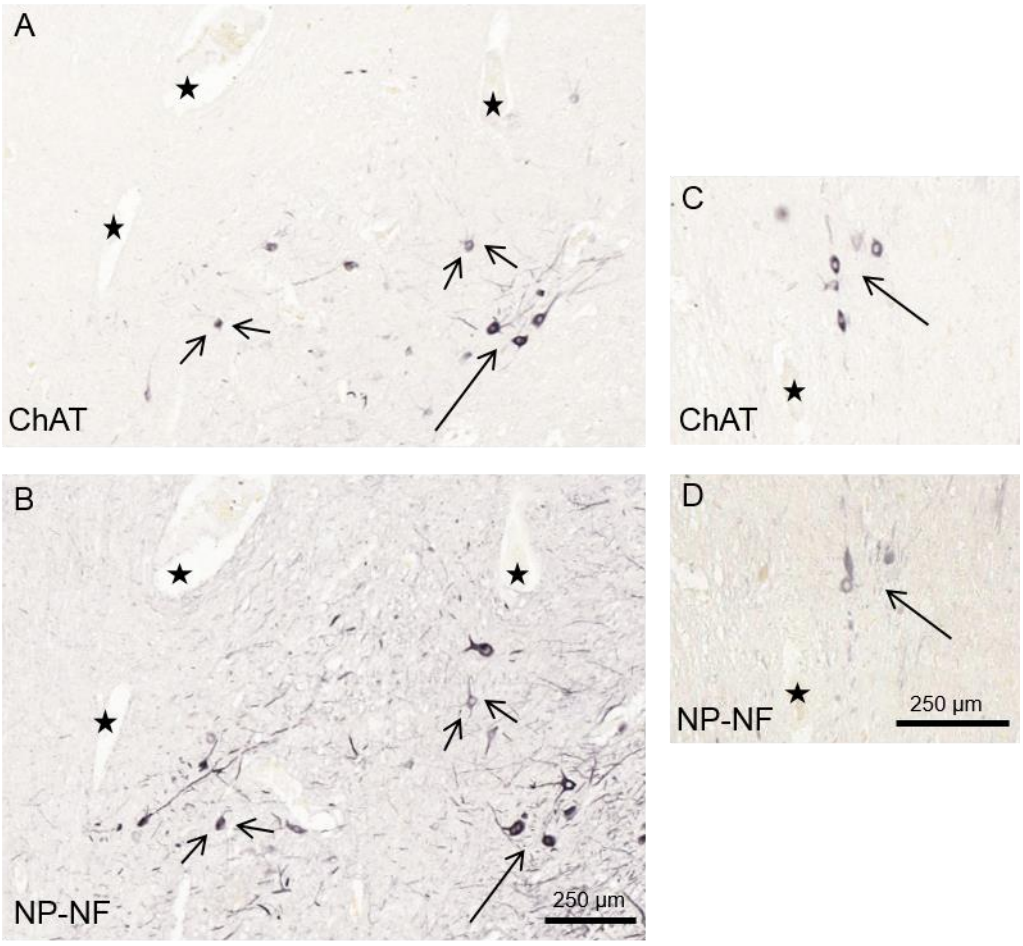

Figure 8. Detailed views of EWpg dorsal group (A,B) and ventral group (C,D) from Figure 7C and D (rectangles), showing double labelled neurons (arrows) for ChAT (A,C) and NP-NF (B,D) in adjacent sections (sections B and D are 10 µm caudal to A and C). For clarity corresponding blood vessels are taged by asterisks in the respective photograph pairs (A and B; C and D). Supplementary immunoreactivity for NP-NF assures that these neurons are representing preganglionic neurons of the ciliary ganglion and not MIF motoneurons.

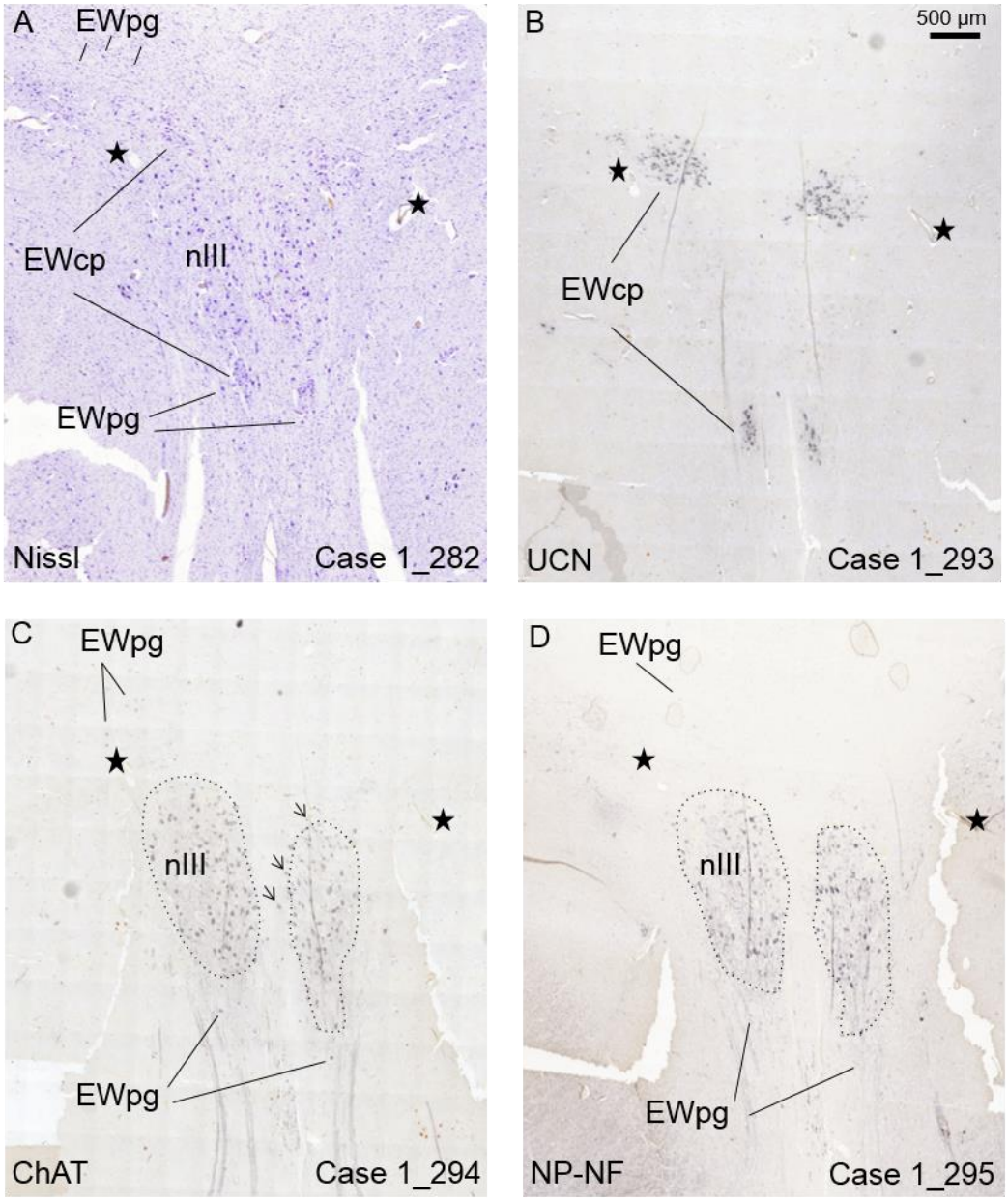

Figure 9. Photographs of neighbouring sections (asterisks in corresponding blood vessels are serving as landmarks) farther rostral to the sections in Figure 7, corresponding to Figure 13 plane E, stained for Nissl, UCN, ChAT and NP-NF to show the cytoarchitecture (A) and the delineation of EWpg from EWcp (B,C) and MIF neurons (C,D). Extraocular muscle motoneurons within nIII and inner eye muscle preganglionic neurons within EWpg are ChAT- (C) and NP-NF-positive (D), neurons of the EWcp are UCN-positve and lack ChAT and NP-NF (B).

ChAT-positive, NP-NF-negative neurons in the immediate vicinity of the dorsomedial border of nIII (see arrows in C) may represent neurons of the MIF group.

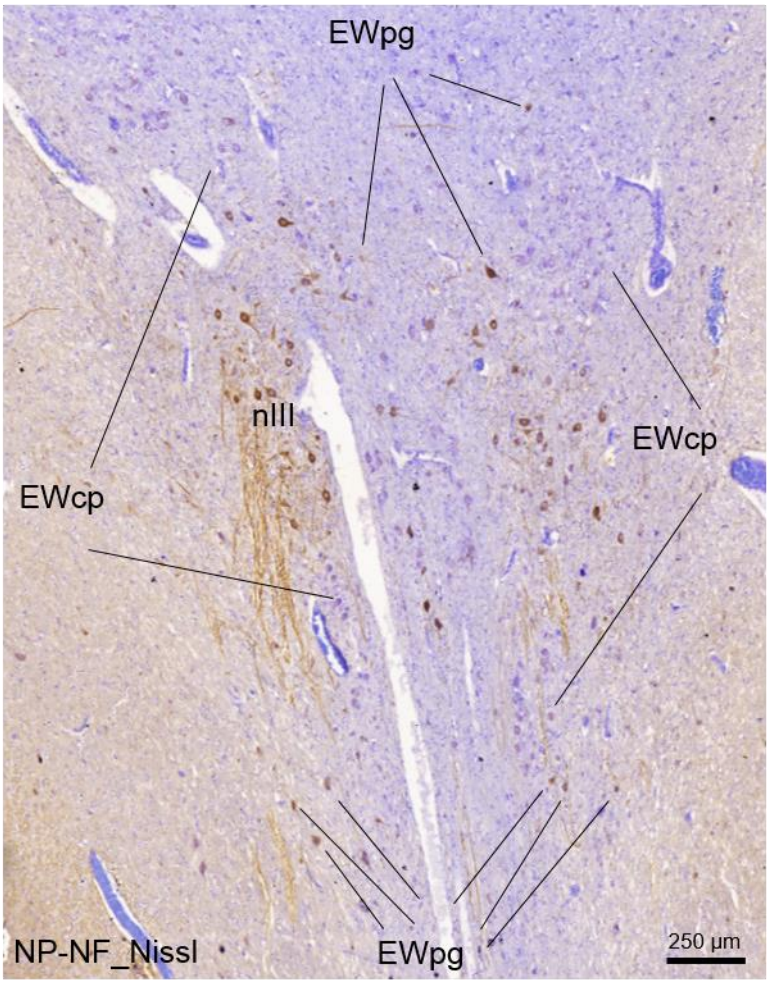

Figure 10. Photograph of a transverse section through the oculomotor nucleus complex at rostral level of nIII, immunostained for NP-NF and counterstained for Nissl to illustrate the dorsal and the ventral EWpg group. The strong NP-NF-immunoreactivity support the assumption that these neurons represent the preganglionic neurons - EWpg.

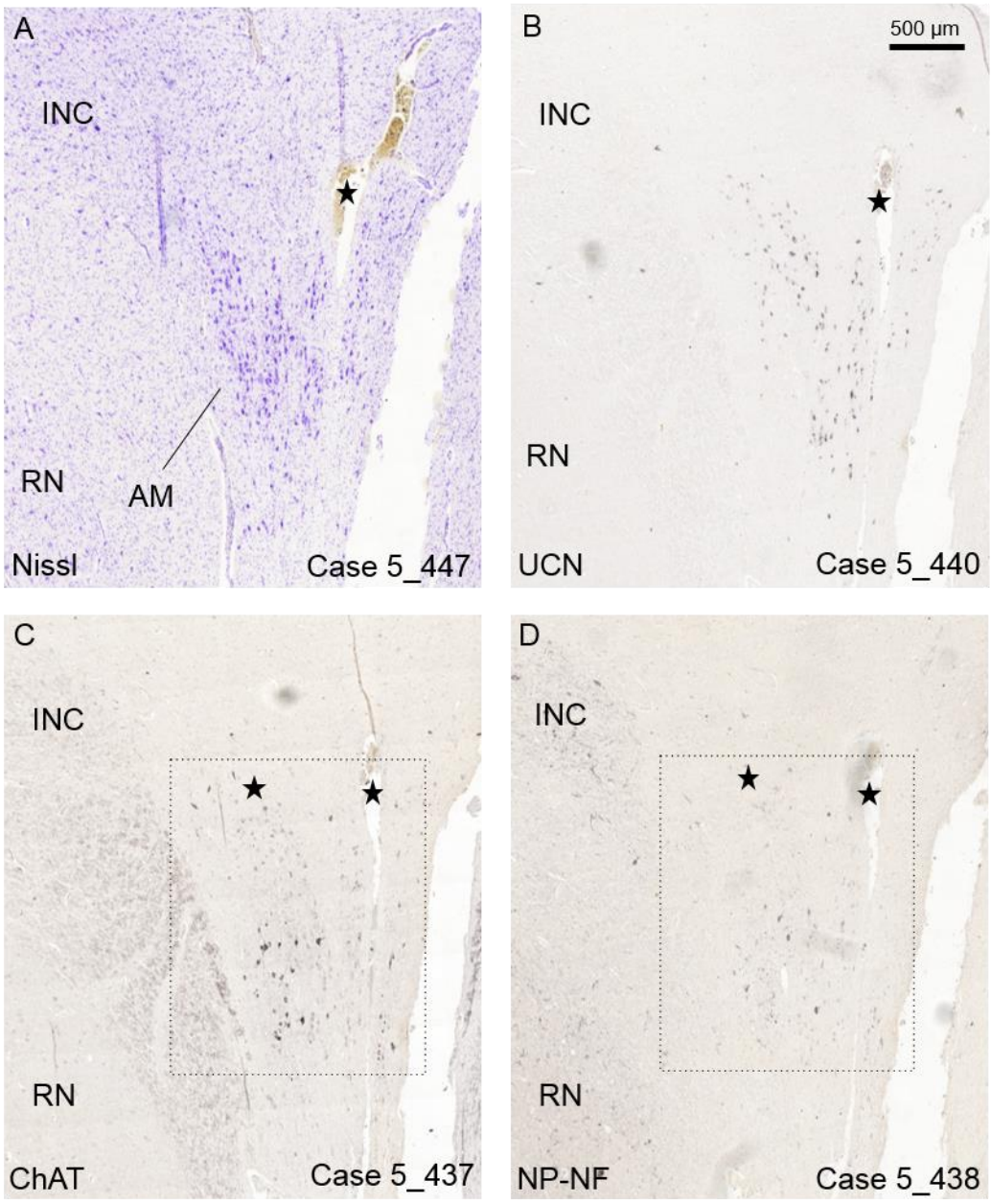

Figure 11. Photographs of neighbouring sections (asterisks in corresponding blood vessels are serving as landmarks) farther rostral then nIII, at the AM level, stained for Nissl, UCN, ChAT and NP-NF to show the cytoarchitecture (A) and the exact content of the AM. The sections illustrate UCN-positive neurons (B) intermingled with ChAT- (C) and NP-NF-positive (D) neurons and demonstrate that the cholinergic neurons within AM are representing parasympathetic preganglionic neurons of the ciliary ganglion.

The squares in C and D mark detailed views of the neurons within AM seen in Figure 12.

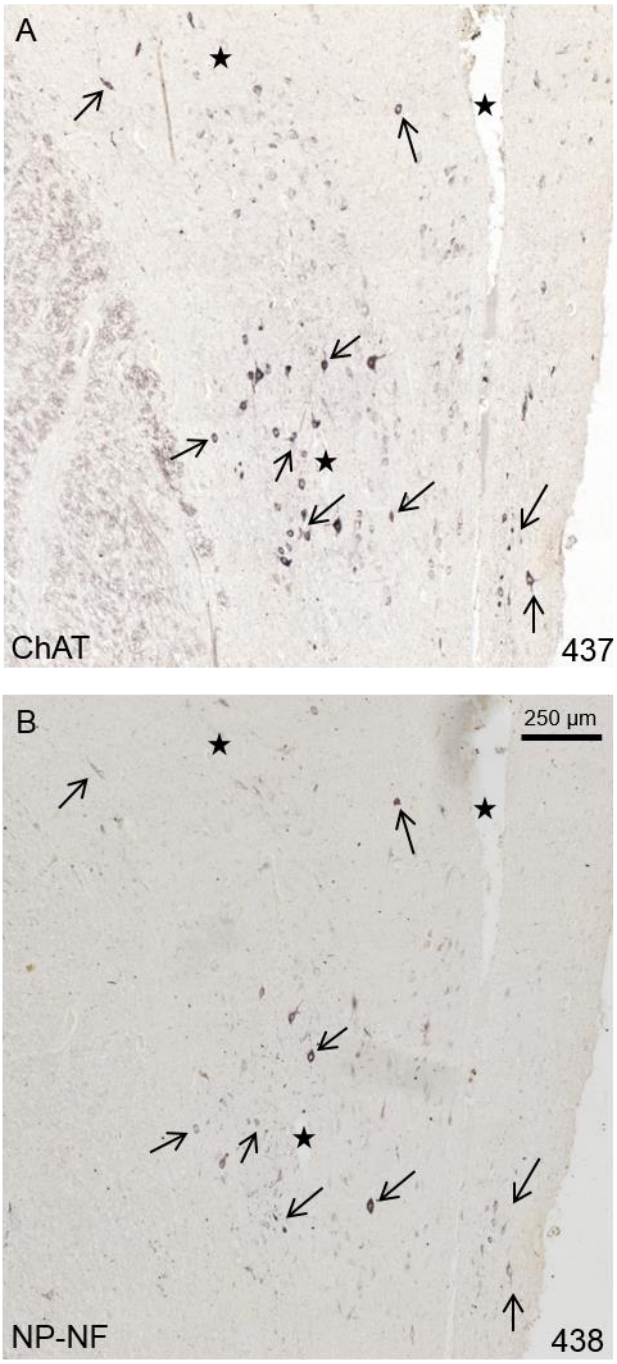

Figure 12. Detailed views of AM from Figure 11C and D (rectangles), showing double labelled neurons (arrows) for ChAT (A) und NP-NF (B) in adjacent sections (section A is 5 µm caudal to B). For clarity corresponding blood vessels are taged by asterisks. Supplementary immunoreactivity for NP-NF assures that the cholinergic neurons within AM are representing preganglionic neurons of the ciliary ganglion.

III.4. Complete population of the preganglionic neurons of EWpg in human

Using the above described characteristics for each functional cell type, the complete distribution of preganglionic neurons in the EWpg in relation to the UCN-positive neurons of the EWcp was determined by plotting the different cell types at several transverse planes from caudal to rostral (Figures 13 and 14).

Coming from caudal the first individual ChAT-positive neurons of EWpg appear dorsal to EWcp at mid-level of the nIII, when the CCN is about to disappear at its rostral end (Figure 14B). This is better seen in Case 2, wherease in Case 1 the cutting angle was different, and did not hit the CCN (see sagittal views of the oculomotor nucleus complex in Figures 13 and 14). Towards rostral levels, the ChAT-positive neurons of EWpg extend as an inconspicuous group over the whole extent of the underlying EWcp (Figure 13B-E and 14B-F). The scattered cholinergic putative preganglionic neurons lie always dorsal to the UCN-positive neurons of the EWcp. But at levels through the rostral half of nIII, the neurons within EWpg are also found ventral to the ventral extension of the UCN-positive neurons within EWcp, as an additional consistent small group of cholinergic neurons (Figure 13D,E; 14E,F).

At the rostral pole of nIII, the cholinergic EWpg neurons intermingle with the UCN-positive neurons and are assigned to the anteromedian nucleus (AM), but are also spilled out dorsally to the boundaries of this nucleus (Figure 13F and 14G). The AM appears as two dorsoventrally oriented cell columns on either side of the midline, which merge to an unpaired column more rostrally (Figure 13F and 14G).

The UCN-positive neurons are confined to the EWcp and AM nuclei as described above but are also spilled outside their borders (Figure 13A-F; 14A-G).

The EWpg extends over a caudo-rostral average distance of approximately 2 mm (see Table 5).

Case	EWpg	nIII
1	1900 µm	2740 µm
2	2352 µm	3248 µm
3	2320 µm	3000 µm
4	1200 µm	1800 µm
5	2000 µm	3200 µm

Table 5. Validation of the extension of EWpg – analysing ChAT and UCN sections from caudal to rostral levels and notating the number of the slide at caudal level starting with the first apearence of cholinergic motoneurons located behind the urocortin-positive neurons. At rostral

level the EWcp and EWpg are intermingled to AM, here notating the slide number where there are almost no cholinergic motoneurons to see.
Validation of the extension of nIII – analysing Nissl and ChAT sections from caudal to rostral levels and notating the number of the slide where nIII first appears at caudal levels and the number of the slide where it disappears at rostral levels.
The variable results rely on the different cutting angle throughout the cases and the fragmentary Case 1 (i.e. Case 4 is almost horizontally cut, Case 1 ends at caudal level at slide number 529 where nIII can be still seen, so nIII should be larger in Case 1).

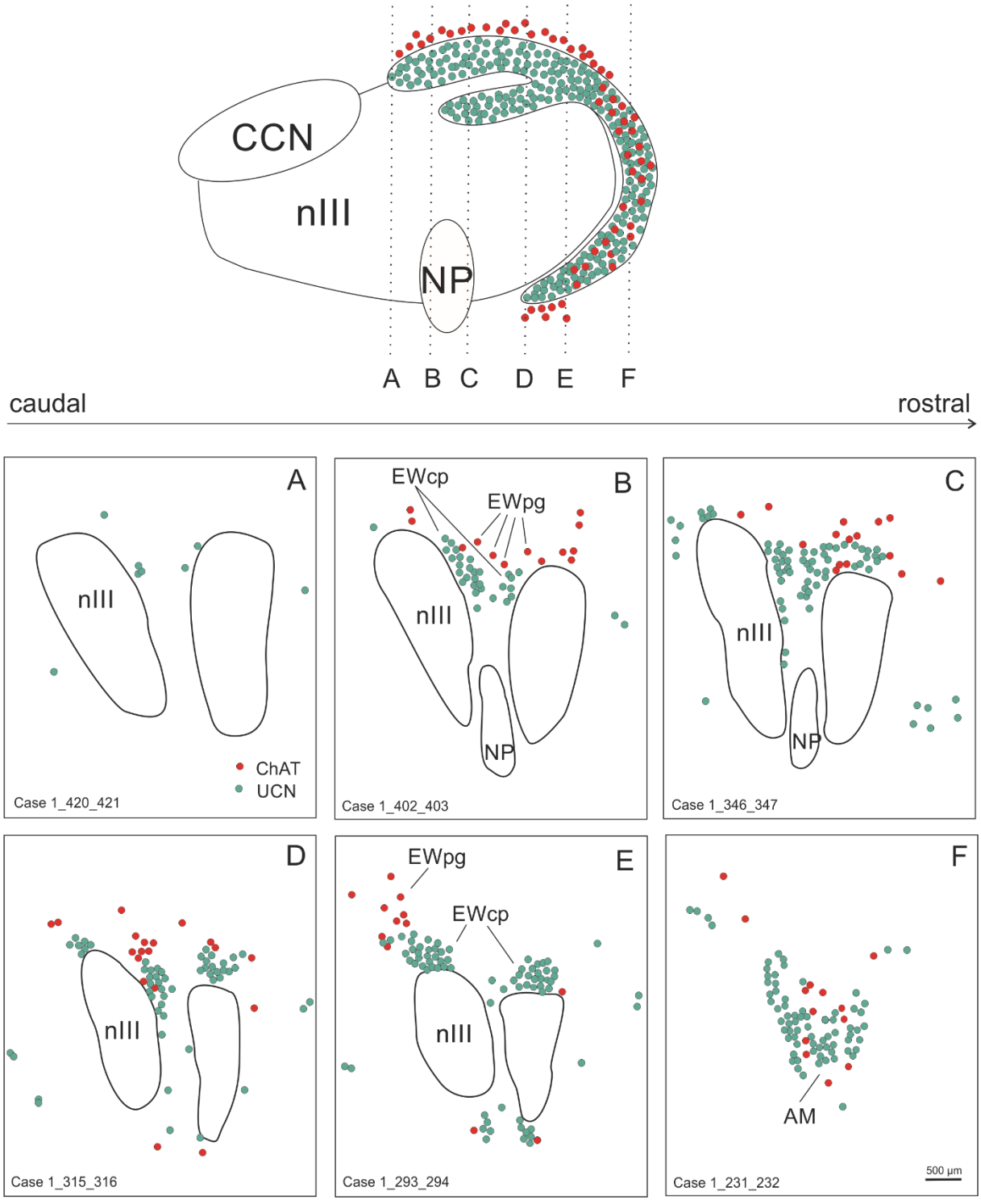

Figure 13 and 14. Schematic drawings of sagittal views of the oculomotor nucleus complex, showing transverse cutting planes from caudal to rostral with the distribution of UCN- and ChAT-positive EW neurons. Each dot represents a labelled cell for either ChAT (red) or UCN (green). The ChAT-positive motoneurons of nIII were not plotted, only the boundaries of this nucleus were drawn.

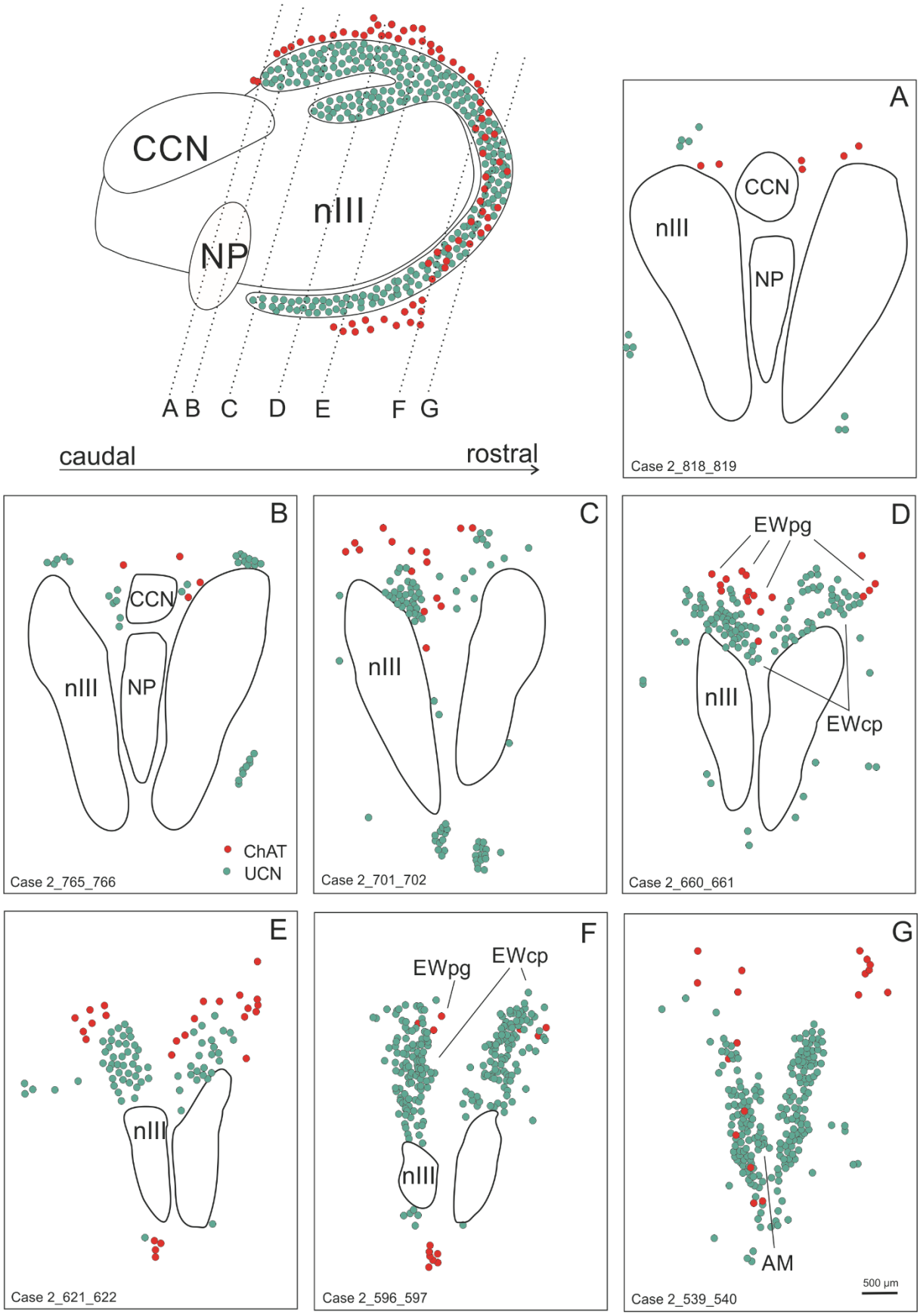
CCN
nIII
NP
A B C D E F G
caudal
rostral
A
CCN
nIII
NP
Case 2_818_819
B
CCN
nIII
NP
ChAT
UCN
Case 2_765_766
C
nIII
Case 2_701_702
D
EWpg
nIII
EWcp
Case 2_660_661
E
nIII
Case 2_621_622
F
EWpg
EWcp
nIII
Case 2_596_597
G
AM
500 µm
Case 2_539_540

Figure 14.

IV. DISCUSSION

IV.1. Edinger-Westphal nucleus

Because of discrepancy along species the term EW was kept for illustrations, found on the nucleus defined by its cytoarchitecture in Nissl-stainings (Olszewski and Baxter's, 1982), but it was augmented by the suffixes "pg" referring to preganglionic, i.e. EWpg and "cp" for central projecting, i.e. EWcp to point out the main population that it consists of (Kozicz et al., 2011).

However in human, unlike in monkey and bird, where the preganglionic neurons of the ciliary ganglion are located within the circumscribed EW, the preganglionic motoneurons are located outside the borders of the Edinger-Westphal nucleus, whereas the neurons within this nucleus are peptidergic, expressing urocortin-1 (Ryabinin et al., 2005; Horn et al., 2008, 2009). There are many different types of urocortin (Ryabinin et al., 2005), in the following it is about urocortin-1, which for the abbreviation UCN will be used for simplicity. UCN is an endogenous ligand for the corticotrophin-releasing factor receptors CRF-1 and CRF-2, and it is involved in the regulation of many behaviors, including anxiety, food intake, alcohol consumption and stress (Gaszner et al., 2004; Pan.W. and A.J.Kastin., 2008; Giardino et al., 2011; Xu et al., 2012). The UCN-positive EW lacks cholinergic markers, which is seen as evidence that it does not contain preganglionic neurons of the ciliary ganglion (Ryabinin et al., 2005; Horn et al., 2008, 2009).

But where exactly are the parasympathetic preganglionic neurons responsible for pupillary constriction and lens accommodation located in human?

Ryabinin et al., 2005 suggested that the EWpg population consists of a compact group of ChAT-positive neurons within the dorsomedial nIII. Horn et al., 2008 controversed Ryabinins suggestion, commenting that this group shows more of the features of extraocular motoneurons and may represent the B-group of medial rectus motoneurons (Büttner-Ennever and Akert, 1981; Büttner-Ennever, 2006). They proposed a consistent group of ChAT-positive neurons located dorsally to the UCN-positive neurons, to be related to the EWpg. These were considered the preganglionic neurons of the ciliary ganglion, based on their similar morphology and histochemical properties with those in monkey (Horn et al., 2008).

IV.2. Complete extent of the EWpg-population

For the first time, the precise localization and the complete extent of the preganglionic motoneurons of the ciliary ganglion was assessed in human, based on staining characteristics similar to those observed in monkey, namely the presence of ChAT- and NP-NF-positive neurons without perineuronal nets (Horn et al., 2008).

Related to lesion and tracing studies in monkey the preganglionic motoneurons supplying the ciliary ganglion are located in the Edinger-Westphal nucleus (Warwick, 1954), this being certified by latest studies (Ostrin and Glasser, 2007; May et al., 2008; McDougal and Gamlin, 2015). This nucleus was termed according to its first descriptors Edinger (1885) and Westphal (1887), who are credited with the discovery of paired cell groups of small cells, dorsomedial to the main oculomotor nucleus, based on human studies. Olszewski and Baxter (1982) defined this nucleus in Nissl-stained sections as a circumscribed cell group dorsomedial to the oculomotor nucleus (nIII) with a ventral extension. Perlia (1889) confirmed these findings, describing in addition a median group of similar small nerve cells, the antero-median nucleus (AM), situated at the rostral end of the nIII. The AM is considered as a rostral prolongation of the traditional EW by some authors (Brouwer, 1918; le Gros Clark, 1926; Adler, 1933), because of the presence of preganglionic neurons of the ciliary ganglion and the similar cytomorphology (Warwick, 1954). But there is insufficient evidence of the real cellular content of the AM in human (Horn et al., 2008).

Surprisingly, the originally suspected function of the nucleus Edinger-Westphal was never further questioned, even if researchers, such as Olszewski and Baxter (1982) stated that the evidence for the role of EW in pupillary constriction and accommodation is scanty. This, presumably also because in non-human primates the preganglionic neurons are actually located in the traditionally EW, as shown by tracer experiments (May et al., 2008b). But only in some species, such as monkey (Akert et al., 1980; Burde and Loewy, 1980; Sun and May, 1993) or bird (Gamlin and Reiner, 1991; Reiner et al., 1991; Cavani et al., 2003), the cytoarchitecturally delineated EW really contains the preganglionic neurons.

In contrast to monkey, where the preganglionic neurons of the ciliary ganglion are confined to the traditional cytoarchitecturally defined EW (May et al., 2008a; Horn et al., 2008), in human the EWpg motoneurons lie scattered along the dorsal and the ventral aspect of the EWcp respectively nIII, but do not form a clearly delineated

nucleus. Moreover the EWpg is not subdivided, it forms a unitary caudorostral population of dispersed motoneurons, but it extends within the AM and dorsal to it.
This findings are consistent with observations in previous studies which described the EWpg population dorsal to the EWcp (Horn et al., 2008, Horn et al., 2009; Kozicz et al., 2011). Also in accordance with the results of the present study is the suggestion of Horn and colleagues (2008) that the cholinergic population within the human AM most likely represent preganglionic neurons.
Furthermore the present study revealed another small group of ChAT-positive neurons ventral to EWcp respectively nIII, which was not described before. Since these neurons show an additional expression of NP-NF, they do not represent MIF motoneurons (Horn et al., 2008) and therefore are here considered part of the EWpg population. Previous studies in cat have shown a similar distribution of preganglionic neurons, dispersing dorsal and ventral to nIII (Erichsen and May, 2002; May et al., 2008a).
At caudorostral levels of the nIII the cholinergic neurons of the EWpg are clearly separated from the adjacent UCN-positive neurons of the EWcp, but rostral to nIII, both populations are intermingled, the part usually assigned to as AM.
An extension of the EWpg neurons within the AM was also seen in monkey and cat (May et al., 2008a). But in the AM of monkey the preganglionic neurons were concentrated in the medial part and enveloped by the UCN-positive neurons (May et al., 2008a). In the cat, the EWpg neurons were found in the AM together with UCN-positive neurons, but also extended lateral and dorsal to this nucleus (May et al., 2008a). In the AM of man, the populations of ChAT- and UCN-positive neurons exhibit a complete territorial overlap.

IV.3. EWpg and EWcp different cell populations with common inputs?

The separation of neurons of the EWcp and EWpg at caudal planes and the mixing of both populations at rostral planes seem to be a general feature in all vertebrate species (Vasconceos et al., 2003; Weitemier et al., 2005; Horn et al, 2008; May et al., 2008a). This distribution pattern could indicate different inputs to both populations at caudal planes. This has been shown for afferent inputs from the central mesencephalic reticular formation (cMRF), that target primarily the preganglionic neurons, but not the UCN-positive neurons of the EWcp (May et al., 2016). Since the cMRF also targets medial rectus motoneurons active during vergence, this input may control the near triad

(Bohlen et al., 2016). On the other hand at rostral planes in the anteromedian nucleus, UCN-positive and cholinergic preganglionic neurons may receive afferents from a common source. A strong input to preganglionic neurons in the EWpg and anteromedian nucleus was found to derive from orexinergic neurons in the hypothalamus, which may control the accommodation and the pupillary system during wakefulness (Schreyer et al., 2009). It is not clear whether orexinergic neurons target only preganglionic neurons, since the UCN-positive neurons were not investigated (Schreyer et al., 2009).

Bakes and colleagues (1990) affirm in their study where they see diminished miotic responses to light in anxious patients that “a possible explanation for the attenuation of the light reflex in anxious patients may lie in the influence of higher centres on the Edinger-Westphal nucleus”, suggesting that the findings may be consistent with a tonically enhanced level of supranuclear inhibition of the Edinger-Westphal nucleus. Knowing that the EWcp is related to stress-, depression- and anxiety-like behavior (Kozicz et al, 2011) and that according to the present findings its neurons are intermingled with the preganglionic neurons within the AM, it is more likely that these different populations share inputs and that this is one reason for diminished miotic responses to light in anxious patients. Moreover, several studies indicate that changes in pupillary response are related to psychiatric diseases, such as anxiety, major depressive disorder and related mood disorders (Fiedorowicz et al., 2012; Roecklein et al., 2013; Graur and Siegle, 2013; Laurenzo et al., 2016).

Put on the fact that the EWcp plays a role in alcohol- and addictive drugs-consumption and several studies are discussing a diminished pupillary light reflex in this cases (Lobato et al., 2013; Hall and Chilcott, 2018), the presumption of an interaction between preganglionic neurons mediating pupillary constriction and the UCN-positive neurons within AM sounds plausible and should be entertained in further studies.

Another finding that also steers in this direction, not only correlated to the pupillary response but also to the lens accommodation, is a finding by Campbell and his colleagues (2001), who affirm that chronic alcohol use can adversely affect subjective static accommodation and also cause slight mydriasis. So, if we assume that the pupillary and ciliary components of the human Edinger-Westphal nucleus are similar to those in cat, namely the rostral portion of the preganglionic population of the ciliary ganglion within and around AM is related to pupil constriction, as more caudal

populations are responsible for lens accommodation (Erichsen and May, 2002), then this suggests that there might be a common input also at caudal levels where EWpg and EWcp population are segregated and do not intermix.

IV.4. EWpg, EWcp and neurodegenerative diseases

Findings that suggested that the traditional defined EW shows noticeable degenerative changes in Alzheimer patients have led researchers to the conclusion that the pupil reflex should be tested for its ability to detect early signs of this degenerative disease (Scinto et al. 1991; Scinto et al. 2001).

But this was obviously an erroneous deduction since the population of neurons that was apparently a preferential target for early tau-load in Alzheimer's disease (Rüb et al., 2001), was actually part of the EWcp, not EWpg. But the fact that the EWcp contains peptidergic neurons that are involved in various functions and habits, such as anxiety and stress responses or regulation of alcohol and food consumption (Ryabinin et al., 2007; Kozicz et al. 2007; Kozicz et al. 2011) may then explain psychiatric syndromes, such as mood swings or depression in Alzheimer's patients (Swaab et al., 2005; Magri et al., 2006; Ryabinin et al., 2012).

Despite the earlier erroneous assumption, pupillary responses are more and more used as biomarkers in neurological diseases such as Alzheimer's disease. The early detection of this disease would allow prompt interventions and a chance to preserve a salubrious brain function (Bittner et al., 2014; Frost et al., 2013a; Frost et al., 2013b). This indicates again that there must be some common input or that the damage to the EWcp population may also somehow affect the parasympathetic fibers arising from the EWpg. Therefore it would be interesting to see, if there is also a damage to the UCN-positive neurons within AM and if so, if the tau-pathology also affects the cholinergic neurons, or whether the changes to pupillary response are due to the involvement of a central cholinergic deficit (Fotiou et al., 2009).

V. CONCLUSION

In summary this study provides a full anatomical description of the exact localization and the complete extent of the EWpg in human.

The inconspicuous cell group of the EWpg extends from mid-level of nIII and overtops it rostrally to continue within the AM, intermingling with the compact, UCN-positive

neuron population of the EWcp, a caudorostral extension of approximately 2 mm. EWpg forms a unitary caudorostral population, in which numerous ChAT- and NP-NF-labelled neurons are scattered dorsal and ventral to the EWcp respectively nIII, with the exception that rostral to nIII it extends into the AM and has occasional outliers dorsal to this nucleus.

The dispersed neurons of the EWpg terminate within the AM, but the UCN-population extends farther rostrally, and its complete extension remains to be evaluated by upcoming reviews. Also the size of preganglionic neuron populations mediating pupillary response and lens accommodation remains to be studied.

Besides, even though the EWpg and EWcp populations show different distribution patterns, they may have considerable overlap in their dendritic fields and some overlap in their somatic distribution. The possibility that these distinct populations share inputs and maybe even a grade of common function must be considered in the future (May et al., 2008a). Moreover, the degree of coexpression of ChAT- and UCN-positive neurons within the AM remains to be explored.

Since in neurodegenerative diseases, such as Alzheimer, the neurons of the EWcp are a prefered target of tau-pathology, but not the preganglionic neurons of EWpg as anticipated earlier, upcoming reviews of Alzheimer patients regarding the tau-pathology observed in the EWcp, should consider that the preganglionic neurons are not situated within this nucleus, instead they can be found dorsal and ventral adjacent to it.

Since the number of research groups studying change in pupil responses related to different diseases is increasing, as is the number of publications, the accurate knowledge about the location of pupil circuitry helps to interprete clinical findings or the topological diagnosis. So in clinical disorders, changes in accommodation and pupil size can now be correlated with the appropriate functional cell group in its complete extension.

In conclusion the present study provides the neuroanatomical basis for clinico-pathological post-mortem analysis addressing the EWpg in cases with pupillary or accommodation dysfunction.

VI. REFERENCES

Akert K, Glicksman MA, Lang W, Grob P, Huber A. 1980. The Edinger-Westphal nucleus in the monkey. A retrograde tracer study. Brain Res 184:491–498.

André Parent; Malcolm B Carpenter. 1996. Carpenter's human neuroanatomy. Baltimore. Williams & Wilkins.

Bachtell RK, Weitemier AZ, Galvan-Rosas A, Tsivkovskaia NO, Risinger FO, Phillips TJ, Grahame NJ, Ryabinin AE. 2003. The Edinger-Westphal lateral septum urocortin pathway and its relation to alcoholinduced hypothermia. J Neurosci 23:2477–2487.

Bakes, A., Bradshaw, C.M., Szabadi, E. 1990. Attenuation of the pupillary light reflex in anxious patients. Br J Clin Pharmacol 30:377–381.

Bittner, D.M.; Wieseler, I.; Wilhelm, H.; Riepe, M.W.; Müller, N.G. 2014. Repetitive pupil light reflex: Potential marker in Alzheimer's disease? J Alzheimer Dis 42:1469–1477.

Bohlen MO, Warren S, May PJ. 2016. A central mesencephalic reticular formation projection to the supraoculomotor area in macaque monkeys. Brain Struct Funct 221:2209-2229.

Bruce G, Wainer BH, Hersh LB. 1985. Immunoaffinity purification of human choline acetyltransferase: comparison of the brain and placental enzymes. J Neurochem 45:611–620.

Burde RM, Loewy AD. 1980. Central origin of oculomotor parasympathetic neurons in the monkey. Brain Res 198:434–439.

Büttner-Ennever JA, Horn AKE. 2014. Olszewski and Baxter's Cytoarchitecture of the Human Brainstem, 3rd edition, Karger, Basel.

Büttner-Ennever JA, Horn AKE, Scherberger H, D'Ascanio P. 2001. Motoneurons of twitch and nontwitch extraocular muscle fibers in the abducens, trochlear, and oculomotor nuclei of monkeys. J Comp Neurol 438:318–335.

Büttner-Ennever JA. 2006. The extraocular motor nuclei: organization and functional neuroanatomy. Prog Brain Res 151:95–125.

Campbell, H., M.J. Doughty, G. Heron & R.G.Ackerley. 2001. Influence of chronic alcohol abuse and ensuing forced abstinence on static subjective accommodation function in humans. Ophthal Physiol Opt 21:197–205.

Cavani, J.A., Reiner, A., Cuthbertson, S.L., Bittencourt, J.C., & Toledo, C.A.B. 2003. Evidence that urocortin is absent from neurons of the Edinger-Westphal nucleus in pigeons. Braz J Med Biol Res *36*(12):1695-1700.

Che Ngwa E, Zeeh C, Messoudi A, Büttner-Ennever JA, Horn AKE. 2014. Delineation of motoneuron subgroups supplying individual eye muscles in the human oculomotor nucleus. Front Neuroanat 8:2.

David H. McDougal, Paul D. Gamlin. 2015. Autonomic Control of the Eye. Compr Physiol 5:439-473.

Eberhorn AC, Ardelenanu P, Büttner-Ennever JA, Horn AKE. 2005. Motoneurons of multiply innervated muscle fibers in extraocular muscles have different histochemical properties than motoneurons of singly innervated muscle fibers. J Comp Neurol 491:352–366.

Eberhorn AC, Büttner-Ennever JA, Horn AKE. 2006. Identification of motoneurons innervating multiply or singly innervated extraocular muscle fibers in the rat. Neuroscience 137:891–903.

Edinger, L. 1885. Über den Verlauf der centralen Hirnnervenbahnen mit Demonstrationen von Präparaten. Arch Psychiat Nervenkr 16: 858–859.

Erichsen JT, May PJ. 2002. The pupillary and ciliary components of the cat Edinger-Westphal nucleus: A transsynaptic transport investigation. Vis Neurosci 19:15–29.

Fiedorowicz JG, Coryell WH, Akhter A, Ellingrod VL. 2012. Chryptochrome 2 variants, chronicity, and seasonality of mood disorders. Psychiatr Genet 22(6):305–306.

Fotiou, D.F.; Stergiou, V.; Tsiptsios, D.; Lithari, C.; Nakou, M.; Karlovasitou, A. 2009. Cholinergic deficiency in Alzheimer's and Parkinson's disease: Evaluation with pupillometry. Int J Psychophysiol 73:143–149.

Gamlin PDR, Reiner A. 1991. The Edinger-Westphal nucleus: sources of input influencing accommodation, pupilloconstriction, and choroidal blood flow. J Comp Neurol 306:425–438.

Gaszner B, Csernus V, Kozicz T. 2004. Urocortinergic neurons respond in a differentiated manner to various acute stressors in the Edinger-Westphal nucleus in the rat. J Comp Neurol 480:170-179.

Giardino WJ, Cocking DL, Kaur S, Cunningham CL, Ryabinin AE. 2011. Urocortin-1 within the centrally-projecting Edinger-Westphal nucleus is critical for ethanol preference. PLoS ONE 6(10):e26997.

Gibbins, I.L. 2012. Peripheral Autonomic Pathways. Chapter 5 in J K Mai & G Paxinos, ed. THE HUMAN NERVOUS SYSTEM. London, UK: Academic Press, pp. 141-185.

Goldstein ME, Sternberger LA, Sternberger NH. 1987. Varying degrees of phosphorylation determine microheterogeneity of the heavy neurofilamentpolypeptide (Nf-H). J Neuroimmunol 14:135–148.

Graur, S. & Siegle. 2013. Pupillary Motility: Bringing Neuroscience to the Psychiatry Clinic of the Future. G. Curr Neurol Neurosci Rep 13: 365.

Hall, C.A., & Chilcott, R.P. 2018. Eyeing up the Future of the Pupillary Light Reflex in Neurodiagnostics. Diagnostics.

Horn, A., A. Eberhorn, W. Härtig, et al. 2008. Perioculomotor cell groups in monkey and man defined by their histochemical and functional properties: a reappraisal of the Edinger-Westphal Nucleus. J Comp Neurol 507:1317–1335.

Ichikawa T, Shimizu T. 1998. Organization of choline acetyltransferasecontainingstructures in the cranial nerve motor nuclei and spinal cord of the monkey. Brain Res 779:96–103.

James Sharpe and Agnes M.F. Wong. 2005. Anatomy and Physiology of Ocular Motor Systems. In N. Miller , N. Newman (Eds.) Walsh & Hoyt Clinical Neuro-Ophthalmology, Chapter 17.

Jiao Y, Sun Z, Lee T, Fusco FR, Kimble TD, Meade CA, Cuthbertson S, Reiner A. 1999. A simple and sensitive antigen retrieval method for free-floating and slide-mounted tissue sections. J Neurosci Meth 93:149-162.

Kardon, R. H. 2005. Anatomy and Physiology of the Autonomic Nervous System. In N. Miller , N. Newman (Eds.) Walsh & Hoyt Clinical Neuro-Ophthalmology, Chapter 14. (6) Williams and Wilkinson.

Kozicz T, Bittencourt JC, May PJ, Reiner A, Gamlin PDR, Palkovits M, Horn AKE, Toledo CAB, Ryabinin AE. 2011. The Edinger-Westphal nucleus: A historical, structural, and functional perspective on a dichotomous terminology, J Comp Neurol 519:1413–1434.

Kozicz, T. 2007. On the role of urocortin 1 in the non-preganglionic Edinger-Westphal nucleus in stress adaptation. Gen Comp Endocrinol 153: 235–240.

Laurenzo SA, Kardon R, Ledolter J, et al. 2016. Pupillary response abnormalities in depressive disorders. Psychiatry Res 246:492–499.

Leigh, R. J., Zee, D. S., & Leigh, R. J. 2006. The neurology of eye movements.

Lobato-Rincón, L.L.; Cabanillas Campos, M.C.; Navarro-Valls, J.J.; Bonnin-Arias, C.; Chamorro, E.; Sánchez-Ramos Roda, C. 2013. Utility of dynamic pupillometry in alcohol testing on drivers. Adicciones 25:137–145.

Magri, F., L. Cravello, L. Barili, et al. 2006. The stress system in the human brain in depression and neurodegeneration. Aging Clin Exp Res 18:167–170.

May PJ, Reiner AJ, Ryabinin AE. 2008a. Comparison of the distributions of urocortin-containing and cholinergic neurons in the perioculomotor midbrain of the cat and macaque. J Comp Neurol 507(3):1300–1316.

May PJ, Sun W, Erichsen JT. 2008b. Defining the pupillary component of the perioculomotor preganglionic population within a unitary primate Edinger-Westphal nucleus. Prog Brain Res 171:97–106.

May PJ, Warren S, Bohlen MO, Barnerssoi M, Horn AKE. 2016. A central mesencephalic reticular formation projection to the Edinger–Westphal nuclei. Brain Struct Funct 221:4073-4089.

Miller, N. R., Newman, N. J., Walsh, F. B., & Hoyt, W. F. 2005. Walsh & Hoyt's clinical neuro-ophthalmology. Philadelphia, PA: Lippincott Williams & Wilkins.

Nieuwenhuys R. 1985. Chemoarchitecture of the Brain. Berlin, Springer Verlag.

Olszewski, J. & D. Baxter. 1982. Cytoarchitecture of the human brain stem. S. Karger. Basel, München, Paris, London, New York, Sydney.

Ostrin LA, Glasser A. 2007. Edinger-Westphal and pharmacologically stimulated accommodative refractive changes and lens and ciliary process movements in rhesus monkeys, Exp Eye Res 84:302–313.

Pan,W. & A.J.Kastin. 2008. Urocortin and the brain. Prog. Neurobiol. 84:148–156.

Reiner A, Erichsen JT, Cabot JB, Evinger C, Fitzgerald ME, Karten HJ. 1991. Neurotransmitter organization of the nucleus of Edinger-Westphal and its projection to the avian ciliary ganglion. Vis Neurosci 6:451–472.

Roecklein K, Wong P, Ernecoff N, Miller M, Donofry S, Kamarck M, Wood-Vasey WM, Franzen P. 2013. The post illumination pupil response is reduced in seasonal affecttive disorder. Psychiatry Res 210(1):150–158.

Rüb U, Del Tredici K, Schultz C et al. 2001. The premotor region essential for rapid vertical eye movements shows early involvement in Alzheimer's disease-related cytoskeletal pathology. Vision Research 41:2149-2156.

Ryabinin AE, Tsoory MM, Kozicz T et al. 2012. Urocortins: CRF's siblings and their potential role in anxiety, depression and alcohol drinking behavior. Alcohol (Fayetteville, NY) 46:349-357.

Ryabinin, A.E. & A.Z. Weitemier. 2006. The urocortin 1 neurocircuit: Ethanol-sensitivity and potential involvement in alcohol consumption. Brain Res Rev 52:368–380.

Ryabinin, A.E., N.O. Tsivkovskaia & S.A. Ryabinin. 2005. Urocortin 1-containing neurons in the human Edinger-Westphal nucleus. Neurosci 134:1317–1323.

Scinto, L.F. M. et al. 1999. Pupil assay and Alzheimer's disease: A critical analysis. Neurology 52(3):673.

Scinto, L.F.M., M. Frosch, C.K. Wu, et al. 2001. Selective cell loss in Edinger-Westphal in asymptomatic elders and Alzheimer's patients. Neurobiol. Aging 22:729–736.

Shaun M. Frost, Yogesan Kanagasingam, Hamid R. Sohrabi, Kevin Taddei, Randall Bateman, John Morris, Tammie Benzinger, Alison Goate, Colin L. Masters and Ralph N. Martins. 2013a. Pupil Response Biomarkers Distinguish Amyloid Precursor Protein Mutation Carriers from Non-Carriers. Current Alzheimer Research 10:790.

Shaun Frost, Yogesan Kanagasingam, Hamid Sohrabi, Pierrick Bourgeat, Victor Villemagne, Christopher C. Rowe, S. Lance Macaulay, Cassandra Szoeke, Kathryn A. Ellis, David Ames, Colin L. Masters, Stephanie Rainey-Smith, Ralph N. Martins and AIBL Research Group. 2013b. Pupil Response Biomarkers for Early Detection and Monitoring of Alzheimer's Disease. Current Alzheimer Research 10:931.

Schreyer S, Büttner-Ennever JA, Tang X, Mustari MJ, Horn AKE. 2009. Orexin-A inputs onto visuomotor cell groups in the monkey brainstem. Neuroscience 164:629-640.

Spencer RF, Porter JD. 2006. Biological organization of the extraocular muscles. Prog Brain Res 151:43–80.

Sternberger LA, Harwell LW, Sternberger N. 1982. Neurotyp: regional individuality in rat brain detected by immunocytochemistry with monoclonal antibodies. Proc Natl Acad Sci U S A 79:1326–1330.

Sternberger LA, Sternberger NH. 1983. Monoclonal antibodies distinguish phosphorylated and nonphosphorylated forms of neurofilaments in situ. Proc Natl Acad Sci U S A 80:6126–6130.

Sun WS, May PJ. 1993. Organization of the extraocular and preganglionic motoneurons supplying the orbit in the lesser galago. Anat Rec 237:89–103.

Swaab, D.F., A.M. Bao & P.J. Luccasson. 2005. The stress system in the human brain in depression and neurodegeneration. Ageing Res Rev 4:141–194.

Tsuchida, U. 1906. Über die Ursprungskerne der Augenbewegungsnerven. Arb hirnanat Inst Zürich. pp. 1-205.

Vasconcelos LAP, Donaldson C, Sita LV, Casatti CA, Lotfi CFP, Wang L, Cadinouche MZA, Frigo L, Elias CF, Lovejoy DA, Bittencourt JC. 2003. Urocortin in the central nervous system of a primate (Cebus apella): sequencing, immunohistochemical, and hybridization histochemical characterization. J Comp Neurol 463:157–175.

Vaughan J, Donaldson C, Bittencourt JC et al. 1995. Urocortin, a mammalian neuropeptide related to fish urotensin I and to corticotropin-releasing factor. Nature 378:287-292.

Warwick R. 1954. The ocular parasympathetic nerve supply and its mesencephalic sources. J Anat 88:71–93.

Wasicky R, Horn AKE, Büttner-Ennever JA. 2004. Twitch and nontwitch motoneuron subgroups of the medial rectus muscle in the oculomotor nucleus of monkeys receive different afferent projections. J Comp Neurol 479:117–129.

Weitemier AZ, Tsivkovskaia NO, Ryabinin AE. 2005. Urocortin 1 distribution in mouse brain is straindependent. Neurosci 132:729–740.

Westphal C. 1887. Über einen Fall von chronischer progressiver Lähmung der Augenmuskeln (Ophtalmoplegia externa) nebst Beschreibung von Ganglienzellengruppen im Bereiche des Oculomotoriuskerns. Arch Psychiat Nervenheilk 98:846-871.

Wilhelm, Helmut. 2011. Disorders of the pupil. Handbook of clinical neurology 102: 427-66.

Xu L, Scheenen WJJM, Roubos EW, Kozicz T. 2012. Peptidergic Edinger–Westphal neurons and the energy-dependent stress response. Gen Comp Endocrinol 177:296-304.

Attachment to materials and methods

Nissl-staining

Colour solution: - 0.5% cresyl violet Bayer Leverkusen + 100 ml distilled water pH 7,4

*Deparaffinization and rehydration

- 15 min. in Xylene
- 15 min. in fresh Xylene

- 10 min. in 100% alcohol
- 10 min. in 96% alcohol
- 10 min. in 90% alcohol
- 10 min. in 70% alcohol

- rinse shortly in distilled water

*Colour

- 0.5% cresyl violet solution for 5 - 10 min.

- sections shortly washed in distilled water

*Dehydration

- 5 min. in 70% alcohol
- 5 min. in 90% alcohol
- 5 min. in 96% alcohol
- 5 min. in 100% alcohol

- 15 min. in Xylene
- 15 min. in fresh Xylene

*Coverslip

Immunostaining for choline acetyltransferase - ChAT

Antibody:

Polyclonal goat anti-choline Acetyltransferase = Chemicon, AB144P (-20°C)

Instructions:

Day 1.

***Pretreatment:**

*Deparaffinization and rehydration of the sections

- 15 min. in Xylene
- 15 min. in fresh Xylene

- 10 min. in 100% alcohol
- 10 min. in 96% alcohol
- 10 min. in 90% alcohol
- 10 min. in 70% alcohol

- rinse shortly in distilled water

Water bath (80°C) for antigen retrieval in formalin-fixed paraffin sections (Jiao et al., 1999)

Midbrain sections were incubated for 15 minutes in 0.01 M sodium citrate buffer pH 8.5 – 9 (sodium citrate [tribasic: dihydrate] ($C_6H_5Na_3O_7.2H_2O$) 2,94g in 900 ml distilled water and titrated with 0.1M sodium hydroxide (2M NaOH : 8g NaOH dissolved in 200 ml distilled water) to a pH of pH 8.5 – 9 and filled up to 1000 ml distilled water), whose temperature (80°C) was maintained by a surrounding water-bath. The water bath was heated in a conventional oven and the temperature (+80°C) was monitored with a thermometer. After heating treatment the sections were cooled to room temperature (RT) before continuing the next steps.

* 0,01M sodium citrate buffer pH 8,5.....**15 min in water bath at +80°C**

(water bath at 80°C turned on 30 min. beforehand, solution in special plastic cuvette)

* cool down in citrate buffer.....15 min at RT

* 1x 0,1M TBS pH 7,6.....5 min

* 2x 0,1M TBS pH 7,6.....5 min

* *Suppression of endogenous peroxidase activity*.....30 min

1% H_2O_2 in 0,1M TBS

* 3x 0,1M TBS pH 7,4.....each for 10 min

* Preincubation.....1h at RT

[*5*% Normal Rabbit Serum + 0,3% Triton in 0,1M TBS pH 7,4]

**** Primary antibody:***….....48 h at 4°C

goat anti-ChAT 1:50

[in *5*% Normal Rabbit Serum + 0,3% Triton in 0,1M TBS pH 7,4]

Day 2.

* 3x 0,1M TBS pH 7,4.....each for 10 min

* Biotinylated *secondary antibody*:.....1h at RT

biot. Rabbit anti-Goat 1:200

[in 0,1M TBS + 2% bovine serum albumin (TBS-RSA)]

* 3x 0,1M TBS pH 7,4.....each for 10 min

* *EAP - extravidin peroxidase - prepared* 30 min before usage.....1h at RT

EAP = Extravidin-Peroxidase 1:1000

[in 0,1M TBS + 2% bovine serum albumin (TBS-RSA)]

* 2 x 0,1M TBS pH 7,4.....je 10 min

* 1x 0,05M TBS pH 7,6….....10 min

*DAB reaction: ..... no direct light radiation on the sections.....10 min

0,025% DAB + 0,015% H_2O_2 in 0,05M TBS pH 7,6

Solution A = 40 mg ammonium nickel in **20ml** 0,05M TBS pH 7,6 **to be optimally filtered**

Solution B = 0,025% DAB = **0,5 ml** von 1% DAB – stock solution in solution A

End-solution C = 10 µl 30% H_2O_2 in solution B

* 3x 0,1M TBS pH 7,4.....each for 10 min

* Distilled water.....……..……5 min

* Allow to dry

* In series of alcohol 70, 90, 96, 100%.....each for 5 min

* 3x Xylene…….....……..……....2x for 5 min und 1x for 15 min

* Coverslip

Immunostaining for non-phosphorylated neurofilaments – NP-NF

Antibody:

Monoclonal mouse anti - non-phosphorylated neurofilaments = Sternberger Monoclonas Incorporated; Cat. Nr. SMI 32 (-20°C)

Instructions:

Day 1.

***Pretreatment:**

*Deparaffinization and rehydration of the sections

- 15 min. in Xylene
- 15 min. in fresh Xylene

- 10 min. in 100% alcohol
- 10 min. in 96% alcohol
- 10 min. in 90% alcohol
- 10 min. in 70% alcohol

- rinse shortly in distilled water

Water bath (80°C) for antigen retrieval in formalin-fixed paraffin sections

Midbrain sections were incubated for 15 minutes in 0.01 M sodium citrate buffer pH 8.5 – 9 (sodium citrate [tribasic: dihydrate] ($C_6H_5Na_3O_7.2H_2O$) 2,94g in 900 ml distilled water and titrated with 0.1M sodium hydroxide (2M NaOH : 8g NaOH dissolved in 200 ml distilled water) to a pH of pH 8.5 – 9 and filled up to 1000 ml distilled water), whose temperature (80°C) was maintained by a surrounding water-bath. The water bath was heated in a conventional oven and the temperature (+80°C) was monitored

with a thermometer. After heating treatment the sections were cooled to room temperature (RT) before continuing the next steps.

* 0,01M sodium citrate buffer pH 8,5.....**15 min in water bath at +80°C**

(water bath at 80°C turned on 30 min. beforehand, solution in special plastic cuvette)

* cool down in citrate buffer.....15 min at RT

* 1x 0,1M TBS pH 7,6.....5 min

* 2x 0,1M TBS pH 7,6.....5 min

* *Suppression of endogenous peroxidase activity*.....30 min

1% H_2O_2 in 0,1M TBS

* 3x 0,1M TBS pH 7,4.....each for 10 min

* Preincubation.....1h at RT

[*5*% Normal Horse Serum + 0,3% Triton in 0,1M TBS pH 7,4]

**** Primary antibody:***….....48 h at 4°C

mouse anti-SMI-32 1:5000

[in *5*% Normal Horse Serum + 0,3% Triton in 0,1M TBS pH 7,4]

Day 2.

* 3x 0,1M TBS pH 7,4.....each for 10 min

* Biotinylated *secondary antibody*:.....1h at RT

biot. Horse anti-Mouse 1:200

[in 0,1M TBS + 2% bovine serum albumin (TBS-RSA)]

* 3x 0,1M TBS pH 7,4.....each for 10 min

* *EAP - extravidin peroxidase - prepared* 30 min before usage.....1h at RT

EAP = Extravidin-Peroxidase 1:1000

[in 0,1M TBS + 2% bovine serum albumin (TBS-RSA)]

* 2 x 0,1M TBS pH 7,4.....je 10 min

* 1x 0,05M TBS pH 7,6….....10 min

*DAB reaction: ..... no direct light radiation on the sections.....10 min

0,025% DAB + 0,015% H_2O_2 in 0,05M TBS pH 7,6

Solution A = 40 mg ammonium nickel in **20ml** 0,05M TBS pH 7,6 **<u>to be optimally filtered</u>**

Solution B = 0,025% DAB = **0,5 ml** von 1% DAB – stock solution in solution A

End-solution C = 10 µl 30% H_2O_2 in solution B

* 3x 0,1M TBS pH 7,4.....each for 10 min

* Distilled water.....5 min

* Allow to dry

* In series of alcohol 70, 90, 96, 100%.....each for 5 min

* 3x Xylene.....2x for 5 min und 1x for 15 min

* Coverslip

Immunostaining for urocortin – UCN

<u>Antibody:</u>

<u>Polyclonal rabbit anti-urocortin = Sigma; U-4757 (not aliquoted and stored at 4°C)</u>

<u>Instructions:</u>

<u>Day 1.</u>

<u>*Pretreatment:</u>

*Deparaffinization and rehydration of the sections

- 15 min. in Xylene
- 15 min. in fresh Xylene

- 10 min. in 100% alcohol
- 10 min. in 96% alcohol
- 10 min. in 90% alcohol
- 10 min. in 70% alcohol

- rinse shortly in distilled water

Water bath (80°C) for antigen retrieval in formalin-fixed paraffin sections

Midbrain sections were incubated for 15 minutes in 0.01 M sodium citrate buffer pH 8.5 – 9 (sodium citrate [tribasic: dihydrate] (C6H5Na3O7.2H2O) 2,94g in 900 ml distilled water and titrated with 0.1M sodium hydroxide (2M NaOH : 8g NaOH dissolved in 200 ml distilled water) to a pH of pH 8.5 – 9 and filled up to 1000 ml distilled water), whose temperature (80°C) was maintained by a surrounding water-bath. The water bath was heated in a conventional oven and the temperature (+80°C) was monitored with a thermometer. After heating treatment the sections were cooled to room temperature (RT) before continuing the next steps.

* 0,01M sodium citrate buffer pH 8,5.....**15 min in water bath at +80°C**

(water bath at 80°C turned on 30 min. beforehand, solution in special plastic cuvette)

* cool down in citrate buffer.....15 min at RT

* 1x 0,1M TBS pH 7,6.....5 min

* 2x 0,1M TBS pH 7,6.....5 min

* *Suppression of endogenous peroxidase activity*.....30 min

1% H_2O_2 in 0,1M TBS

* 3x 0,1M TBS pH 7,4.....each for 10 min

* Preincubation.....1h at RT

[*5*% Normal Goat Serum + 0,3% Triton in 0,1M TBS pH 7,4]

**** Primary antibody:***….....48 h at 4°C

rabbit anti-Urn 1:6000

[in 5% Normal Goat Serum + 0,3% Triton in 0,1M TBS pH 7,4]

Day 2.

* 3x 0,1M TBS pH 7,4.....each for 10 min

* Biotinylated *secondary antibody*:.....1h at RT

biot. Goat anti-Rabbit 1:200

[in 0,1M TBS + 2% bovine serum albumin (TBS-RSA)]

* 3x 0,1M TBS pH 7,4.....each for 10 min

* *EAP - extravidin peroxidase - prepared* 30 min before usage.....1h at RT

EAP = Extravidin-Peroxidase 1:1000

[in 0,1M TBS + 2% bovine serum albumin (TBS-RSA)]

* 2 x 0,1M TBS pH 7,4.....je 10 min

* 1x 0,05M TBS pH 7,6….....10 min

*DAB reaction: ..... no direct light radiation on the sections.....10 min

0,025% DAB + 0,015% H_2O_2 in 0,05M TBS pH 7,6

Solution A = 40 mg ammonium nickel in **20ml** 0,05M TBS pH 7,6 **<u>to be optimally filtered</u>**

Solution B = 0,025% DAB = **0,5 ml** von 1% DAB – stock solution in solution A

End-solution C = 10 µl 30% H_2O_2 in solution B

* 3x 0,1M TBS pH 7,4.....each for 10 min

* Distilled water.....……5 min

* Allow to dry

* In series of alcohol 70, 90, 96, 100%.....each for 5 min

* 3x Xylene……....2x for 5 min und 1x for 15 min

* Coverslip

Eidesstattliche Versicherung/Affidavit

Name, Vornamen: **Valeanu, Laura Ioana**

Hiermit versichere ich an Eides statt, dass ich die vorliegende Dissertation: **„The localization and complete extent of the newly defined preganglionic Edinger-Westphal nucleus (EWpg) in human“** selbstständig angefertigt habe, mich außer der angegebenen keiner weiteren Hilfsmittel bedient und alle Erkenntnisse, die aus dem Schrifttum ganz oder annähernd übernommen sind, als solche kenntlich gemacht und nach ihrer Herkunft unter Bezeichnung der Fundstelle einzeln nachgewiesen habe.

I hereby confirm that the dissertation: **„The localization and complete extent of the newly defined preganglionic Edinger-Westphal nucleus (EWpg) in human“** is the result of my own work and that I have only used sources or materials listed and specified in the dissertation.

München, den Munich, date	Unterschrift / signature
20.05.2020	Laura Ioana Valeanu

Acknowledgements

Hereby I want to express my regards and thanks especially to Prof. Dr. rer. nat. Anja Horn-Bochtler for her undeterminable support, amazing teaching skills, prompt advice and flexibility. Dear Anja, you have always been an inspiration for me and I cannot express how greatful I am to have had the opportunity to work with a wonderful supervisor like you.

I also want to thank here Ahmed Messoudi and Christine Unger for introducing me to the laboratory technics and for guiding me to improve my staining skills and get accurate results. Furthermore I am appreciative to Karoline Lienbacher, Miriam Barnerßoi and Christina Zeeh for embracing me in the delightful oculomotor team. Many thanks for your extraordinary support and for sharing your wide-ranging knowledge, experience and valuable ideas in all this time. I would also like to kindly thank Prof. Dr. med. Jens Waschke, head of the Institution for his great support.

Particulary I want to thank my spouse Radu Florian, for his love, his supportive and limitless encouragement and for conveying me the necessary peace of mind and equilibrium to complete this sublime work.

Moreover I want to warmly thank my family and especially my mother PhD Dr. Valeria Valeanu for her firepower and her financial support during my studies at the Ludwig-Maximilians-University of Munich.

Last but not least I want to show my gratitude to Sally Wood-Lamont and Mariana Blidaru from the Romanian National Paralympic Committee, for their financial support and also to my Ski Coach Manfred Auer and my Ski Technician Hermann Habersatter for accompanying me on this journey back to the top of the Paralympic Alpine Skiing, this way offering me the mandatory support to accomplish this glorious work.